Sl. No.	IIT Ropar List of Recent Publications with Abstract Coverage: February, 2022
1.	A fully analytical model of a box solar cooker with sensible thermal storage S Verma, S Banerjee, R Das - Solar Energy, 2022 **Abstract**: A box-type solar cooker supplemented with a sensible heat storage medium (for nocturnal cooking) has been analytically investigated. Unlike other available analytical studies where the relevant time interval is divided into a large number of smaller intervals and time marching is conducted numerically, here, a series of sinusoidal functions for time-dependent system driving parameters is considered via which fully closed form solutions are derived for cooking fluid and storage medium temperatures as functions of time. Here, the influences of storage medium mass and two newly defined parameters: cooking vessel area fractions for day and night cooking are investigated. Results reveal that the system's performance increases with reduced storage medium mass and increased night cooking vessel area fraction. It is inferred that increased area of vessel at day, on one hand reduces day cooking time, while on other hand, raises the night cooking time, and therefore, its value must be selected by considering these two effects. Further, the calculations also predict that the maximum storage medium temperature is not attained at the end of sunshine period, but some time before it. Thus, charging of this medium must be stopped at the time beyond which its temperature begins to decrease. This work therefore lays down guidelines for the design of box type solar cookers with sensible thermal storage and can prove useful in predicting the appropriate time at which charging of storage medium must be ceased and also in selecting the cooking vessel dimensions for both day and night cooking.
2.	A generalization of multifractional Brownian motion N Gupta, A Kumar, N Leonenko - Fractal and Fractional, 2022 **Abstract**: In this article, some properties of multifractional Brownian motion (MFBM) are discussed. It is shown that it has persistence of signs long range dependence (LRD) and persistence of magnitudes LRD properties. A generalization called here nth order multifractional Brownian motion (n-MFBM) that allows to take the functional parameter H(t) values in the range (n−1,n) is discussed. Two representations of the n-MFBM are given and their relationship with each other is obtained.
3.	A Multi-turn Coil Antenna with Non-uniform Clustered Turns Optimized using Q-assisted MMSE Procedure to Enhance Misalignment Tolerance in WPT Systems A Bharadwaj, A Sharma, CC Reddy - IEEE Transactions on Antennas and Propagation, 2022 **Abstract**: In this paper, an optimized non-uniformly distributed turn coil antenna is proposed to mitigate the lateral misalignment problem in wireless power transfer (WPT) systems. The proposed Q-assisted H-field forming technique is analytically implemented using a Minimum Mean Square Error (MMSE) based algorithm. This results in an optimized transmitter coil with clustered turns achieving a widespread uniformity of the H-field in the receiver working region. The proposed optimal design shows a consistent mutual inductance and power transfer efficiency (PTE) irrespective of the receiver misalignment which is realized using the circuit parameters. The analytical and simulated results of the proposed transmitter coil designed using the Q-assisted MMSE-based H-field forming technique is experimentally verified. The misalignment tolerance of the proposed antenna is improved over the existing design by 224The proposed design proves its advantage to realize misalignment tolerant wireless charging platforms for

	WPT applications.
4.	A PMU assisted cyber attack resilient framework against power systems structural vulnerabilities S De, R Sodhi - Electric Power Systems Research, 2022 **Abstract**: In this work, a comprehensive cyber-attack resilient framework is developed which combats the structural vulnerabilities in the smart grids with the help of strategically placed Phasor Measurement Units (PMUs). To this end, a novel Hybrid Betweenness Centrality (HBC) measure is proposed which effectively identifies the most critical lines in a system. In order to make the system resilient against any false data injection attacks on these vulnerable lines, a novel objective function is developed for strategic PMU placements in the system. The optimal PMU placement results provide the minimal sets of measurements that need to be made secured to protect the state variables against any kind of data integrity types of attacks. The efficacy of the proposed framework is demonstrated on the IEEE 14-bus system and the New England (NE) 39-bus system throught various case studies.
5.	A Robust Training Signal Generator for Trainable Memristive Digital to Analog Converter S Shivdeep, SK Vohra, N Goel, DM Das - IEEE International Symposium on Smart Electronic Systems, 2021 **Abstract**: There is a perpetual need of evolution in data converters to cater the demand of high speed and accurate data acquisition and processing. The trainable neural data converters can be trained using supervised learning techniques to produce precise data conversions. Such data converters are PVT immune and can be trained in real time using on-chip training signal generators. A trainable digital to analog converter needs accurate labeled analog signals as training signal. This paper proposes a CMOS-memristor hybrid training signal generator circuit and a memristive variable slope ramp generator circuit design. Proposed architecture is PVT immune and robust against mismatches and manufacturing imprecision in circuit component parameters. Proposed design is scalable to produce training signal for N-bit digital to analog converters. Proposed work is implemented and validated in standard CMOS 180nm technology node with SPICE model for the memristor.
6.	A simple yet efficient approach for electrokinetic mixing of viscoelastic fluids in a straight microchannel C Sasmal - Scientific Reports, 2022 **Abstract**: Many complex fluids such as emulsions, suspensions, biofluids, etc., are routinely encountered in many micro and nanoscale systems. These fluids exhibit non-Newtonian viscoelastic behaviour instead of showing simple Newtonian one. It is often needed to mix such viscoelastic fluids in small-scale micro-systems for further processing and analysis which is often achieved by the application of an external electric field and/or using the electroosmotic flow phenomena. This study proposes a very simple yet efficient strategy to mix such viscoelastic fluids based on extensive numerical simulations. Our proposed setup consists of a straight microchannel with small patches of constant wall zeta potential, which are present on both the top and bottom walls of the microchannel. This heterogeneous zeta potential on the microchannel wall generates local electro-elastic instability and electro-elastic turbulence once the Weissenberg number exceeds a critical value. These instabilities and turbulence, driven by the interaction between the elastic stresses and the streamline curvature present in the system, ultimately lead to a chaotic and unstable flow field, thereby facilitating the mixing of such viscoelastic fluids. In particular, based on our proposed approach, we show how one can use the rheological properties of fluids and associated fluid-mechanical phenomena for their efficient

	mixing even in a straight microchannel.
7.	A surface modification approach to overcome wetting behaviour of gallium based liquid metal droplets R Kumar, V Ghai, AK Sahani - IEEE Transactions on Nanotechnology, 2022 **Abstract**: Gallium based eutectic alloys are one of the promising substitutes of mercury. These alloys are nontoxic and environment friendly and have similar or equivalent properties as that of mercury. These alloys exhibit good electrical and thermal properties. However, these alloys form oxides when in contact with oxygen atoms. Due to this, the material inertness deteriorates, which renders them unsuitable for those applications where the mobility of the fluid is a valuable factor, such as in thermometers and blood pressure monitoring devices. There are few methods reported to remove the oxide layer from the surface of the gallium-based alloys, like acid and base treatment prior to use, but all these methods are not durable and longlasting. Here in this work, we report gallium oxide coating as a simple approach to convert mercury manometer glass tube, which has glass as a substrate to a nonwetting surface against surface-oxidized gallium- based liquid metal alloys. These alloys form an oxidized layer in ambient air (O2 1ppm) and show stickiness to almost all surfaces that impact the residue-free movement of the liquid metal droplets. Herein, the physical vapor deposition technique was used for gallium oxide coating on substrates such as silicon wafer and glass slide. Moreover, various characterizations were carried out to support our outcomes. This method does not require any micro/nano machining or specific nanoscale surface topology. The contact angle was measured with or without coated gallium oxide film on the glass substrate, and the static contact angle (c.a.) 137.69 and with bared glass c.a. 94.30.
8.	A Systematic Review on Muscle Stimulation Techniques N Kashyap, VK Baranwal, B Basumatary, R Bansal, A Sahani - IETE Technical Review, 2022 **Abstract**: The conventional procedure in retraining a muscle has been physiotherapy, but persistence is required, which often proves to be a limitation in most patients. The electrical stimulation technique has great potential in comparison to conventional methods that are employed in retraining muscles. The neuromuscular electrical stimulation method uses a device that sends electrical impulses to neurones. This input causes the muscle to contract. It can be used to re-educate or retrain a muscle. In this review article, how different types of stimulation strategies can be used for re-educating muscles in different diseased conditions is studied. The force and quality of the muscle contraction depend upon several parameters such as frequency, amplitude, pulse duration and waveforms of stimuli. The Analysis of parameters involved in different stimulation techniques can help in understanding how a particular muscle can be stimulated in different diseased conditions. There are several studies that have reported the efficacy of muscle stimulation strategies. In this review, we investigated 30 research studies that used the muscle stimulation method for re-educating muscle and discussed many considerations in context to muscle stimulation techniques: the stimulation strategies and parameters, electrodes and results. With this review, we investigated a potential intervention for re-educating muscle and tried to recognise the limitations and benefits of the current strategies involved.
9.	Algorithm to Avoid Normal Tissue Sacrifice and Thermal Injury of Neighbouring Organs During Radiofrequency Ablation of HCC Tumours Treated Using a Multi-Tine Electrode With Separately Controlled Tines M Dhiman, R Repaka - ASME International Mechanical Engineering Congress and Exposition, 2021

	Abstract: Radiofrequency ablation of Hepatocellular Carcinomas lacks electrode level feature to (a) avoid the risk of thermal injury to the neighbouring organs and (b) avoid the sacrifice of normal hepatic tissue. The absence of such a feature causes additional intrusion of the human body to overcome the first problem, while there is no solution for the latter problem. An algorithm has been developed and implemented using an unconventional multi-tine RFA electrode to incur ablations specific to the shape and position of target tumours to solve these problems. Further, this algorithm can suggest the best insertion angle for the trocar, such that minimum normal tissue is sacrificed. This suggestion is made quickly with the help of a pre-simulated database. For verification of the algorithm, pre-segmented tumours have been used as inputs and damages incurred with and without algorithm have been compared.
10.	An Autoencoder Based Approach to Enable High Fidelity Video Conferencing over Low Bandwidth Networks S Kulshrestha, A Jain, A Sahani - IEEE 18th India Council International Conference, 2021 **Abstract**: Data lagging and distortion has been the issue for the majority of us since the usage of online video conferencing platforms has become a routine of our daily life. In this paper, we attempted to design a solution for this by specifically for the image part of the videos, by building a convolution neural network based autoencoder, which will compress the images being sent from one end to another in a batch of 5 frames, and stretch it back to its original size on the receiver end. We calculated the accuracy and loss obtained for the same for comparison purposes.
11.	An overview of dimensions and dimensions badge V Jamwal, H Kumar - Library Hi Tech News, 2022 **Abstract**: Purpose Research assessment has long been important for directing research funding, rationalizing research organizations and enhancing productivity, including concentrating on specialized subjects. But due to a lack of data, research assessment procedures centered on simple indicators that solely included publications and their citation counts. The Dimensions is one such prodigy of technological evolution like the internet in discovering the research data metrics. Design/methodology/approach This paper outlines Dimensions, the emergence of Dimensions by partnering with various development partners into a single robust platform and provides directions on implementing a free tool for research insights: Dimensions badge. Findings The Dimensions platform for research insights pulls together data on financing, publications, policy, patents and grants. Originality/value This tool is freely available to libraries worldwide.
12.	Aza-Oxyallyl Cation Driven 3-Amido Oxetane Rearrangement to 2-Oxazolines: Access to Oxazoline Amide Ethers IM Taily, D Saha, P Banerjee - The Journal of Organic Chemistry, 2022 **Abstract**: Herein, we report a highly facile and unprecedented activation of 3-amido oxetanes to

	synthesize 2-oxazoline amide ethers using a transient electrophilic aza-oxyallyl cation as an activating as well as an alkylating agent under mild reaction conditions. The aza-oxyallyl cation driven intramolecular rearrangement of 3-amido oxetanes to 2-oxazolines is the hallmark of this transformation and is a new addition to the reactivity profile of aza-oxyallyl cations. 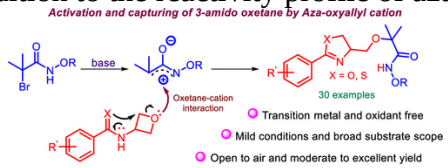
13.	Bifunctional Tungsten-Doped $Ni(OH)_2$/NiOOH Nanosheets for Overall Water Splitting in an Alkaline Medium D Rathore, A Banerjee, S Pande - ACS Applied Nano Materials, 2022 **Abstract**: The development of a cost-effective and proficient bifunctional electrocatalyst is highly fascinating. Herein, we have synthesized a tungsten (W^{6+})-doped vertically grown nanosheet-like structure of $Ni(OH)_2$/NiOOH on carbon cloth for hydrogen evolution reaction (HER) and oxygen evolution reaction (OER) activity in KOH solution. Doping with W^{6+} ions in $Ni(OH)_2$/NiOOH is performed by electrodeposition, followed by the hydrothermal method. Various amounts of the dopant (W^{6+}) are used to confirm the role of W, but the $W_{0.1}Ni(OH)_2$/NiOOH nanosheet shows the highest efficiency in electrocatalysis. The surface composition and the oxidation state of the developed electrocatalyst are confirmed by inductively coupled plasma atomic emission spectroscopy and X-ray photoelectron spectroscopy analyses. After doping, the lattice suffers a tensile strain, which is confirmed by Raman and X-ray powder diffraction analyses. Field emission scanning electron microscopy and transmission electron microscopy analyses confirm the nanosheet morphology of $W_{0.1}Ni(OH)_2$/NiOOH. The electrocatalyst, $W_{0.1}Ni(OH)_2$/NiOOH, has a lower value of overpotential of 56 and 293 mV to obtain current densities of 10 and 50 mA/cm2 for HER and OER, respectively, in a basic medium. The corresponding Tafel slope values are 63.5 and 48.2 mV dec–1 for HER and OER, respectively. In $W_{0.1}Ni(OH)_2$/NiOOH, the W^{6+} ion is a d0 system that behaves as a strong Lewis acid and helps in electron pulling from Ni^{2+} ions, which facilitates the formation of Ni_{3+} ions as an active site for HER and OER. The electron pulling nature of the W^{6+} ion is further confirmed from Bader's charge analysis. Moreover, the synergistic effect between Ni^{2+} and W^{6+} ions plays an important role in a higher electrocatalytic efficiency. Density functional theory calculations revealed an increase in the Gibbs free energy of H adsorption in the presence of W, suggesting an enhanced HER activity for $W_{0.1}Ni(OH)_2$/NiOOH. 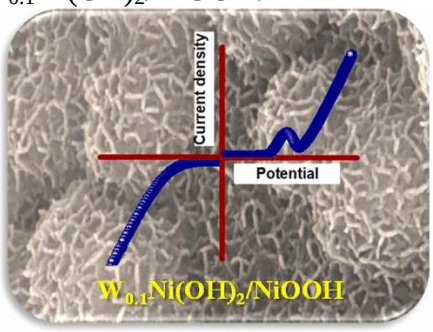
14.	Catalytic steam reforming of simulated bio-oil for green hydrogen production using highly active $LaNi_xCo_{1-x}O_3$ perovskite catalysts PP Singh, N Nirmalkar, T Mondal - Sustainable Energy & Fuels, 2022

	Abstract: Catalytic steam reforming (SR) of agricultural waste derived bio-oil for hydrogen production is an unique technology, offering twin benefits of waste management and sustainable energy production. In the present study, a series of $LaNi_xCo_{1-x}O_3$ perovskite catalysts (x = 0, 0.2, 0.4, 0.5, 0.6, 0.8 and 1.0) were used for the steam reforming of simulated bio-oil to produce green hydrogen. The fresh and spent catalysts were characterized by various characterization techniques such as X-ray diffraction (XRD), H_2-temperature programmed reduction (TPR), BET (Brunauer–Emmett–Teller), Raman spectroscopy, thermogravimetric analysis (TGA) and scanning electron microscopy (SEM). The effects of variation of reaction temperature, Ni and Co species composition, steam to carbon molar ratio (SCMR), and weight hourly space-time (WHST) on gaseous product yield and simulated bio-oil conversion were evaluated using a fixed catalytic bed reactor unit. The results revealed that $LaNi_{0.5}Co_{0.5}O_3$ exhibited the best catalytic activity (83% hydrogen yield and 95% conversion) towards hydrogen production, among all other combinations of $LaNi_xCo_{1-x}O_3$ catalysts at 650 °C and a space-time and SCMR of 18.4 kg_{cat} h $kmol_{bio\text{-}oil}^{-1}$ and 2.7 respectively for 12 h. Moreover, a catalyst deactivation study performed using TG, Raman, and SEM analysis revealed that the deactivation was primarily due to two types of coke (amorphous and filamentous carbon) deposition.
15.	Cavitation erosion mechanisms of HVOF-sprayed Ni-based cermet coatings in 3.5% NaCl environment NK Singh, G Vinay, ASM Ang, DK Mahajan, H Singh - Surface and Coatings Technology, 2022 **Abstract**: Monel K-500 is a nickel-based alloy that is a widely used material in industries like hydraulic, chemical and marine. In its marine application, such as in seawater, Monel alloy suffers from high cavitation and corrosion. In one of the approaches to control these degradations, thermal spray coatings are recommended to enhance the resistance against these degradations. The current study assesses the synergic effect of cavitation erosion (CE) and corrosion on two HVOF-sprayed nickel-based cermet coatings, WC-10Ni5Cr (WC-NiCr) and WC-18Hastelloy C (WC-H), on Monel K-500 substrate. CE tests were conducted for 15 h in a corrosive (3.5% NaCl) environment. It was observed that WC-NiCr coating reduced the CE losses in Monel alloy by 45%. In pure cavitation (DI water) conditions, the better CE of a coating originates from its better combination of microhardness and indentation toughness. Whereas, in a corrosive medium, the CE behavior of a coating depends upon its electrochemical properties too. Electrochemical corrosion test on both the coatings revealed that WC-NiCr coating had better corrosion results than that of WC-H coating due to its higher corrosion potential (Ecorr) value and slightly lower corrosion current density which may influence the CE performance of the investigated coatings. In-depth study of the erosion mechanism for each of the coatings was conducted using Scanning Electron Microscopy (SEM). It was observed that due to the effect of the corrosive medium, several pits and pores were generated over the coating surface. These defects provided additional nucleation sites for CE in the coatings resulting in a high level of erosion losses in the coatings. Considering the effects of cavitation and corrosion simultaneously, HVOF-sprayed WC-NiCr coating is recommended to enhance the cavitation-corrosion resistance in Monel K-500 alloy.
16.	Cellulose-reinforced poly (ethylene-co-vinyl acetate)-supported Ag nanoparticles with excellent catalytic properties: synthesis of thioamides using the Willgerodt-Kindler reaction A Singh, S Saini, N Singh, N Kaur, DO Jang - RSC Advances, 2022 **Abstract**: Cellulose, a bio-derived polymer, is widely used in food packaging, dye removal, coatings, and solid-supported catalysis. Heterogeneous catalysts play a critical role in

	environmental remediation. In this context, the demand for green and cost-effective catalysts has rapidly increased. In this study, cellulose was extracted from rice straw, and a highly active solid-supported catalytic model was developed. First, cellulose was conjugated with poly(ethylene-co-vinyl acetate) (PEVA), and then Ag nanoparticles (AgNPs) were inserted into the cellulose–PEVA composite. The process involved the reduction of AgNPs in the presence of sodium borohydride. The fabricated hybrid catalyst was characterized using Fourier-transform infrared spectroscopy, scanning electron microscopy, energy dispersive X-ray, and powder X-ray diffraction. Thereafter, the obtained hybrid was used as a catalyst for the Willgerodt–Kindler reaction of aromatic aldehydes, amines, and S8 to synthesize thioamides with excellent yields. The developed catalytic system exhibited high stability and recyclability. Moreover, the mechanical properties of the hybrid catalyst were evaluated using tensile strength and impact tests. RGB analysis of digital images was also performed to investigate the primary components of the catalyst. 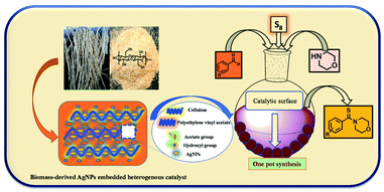
17.	Climate warming and dispersal strategies determine species persistence in a metacommunity A Narang, PS Dutta - Theoretical Ecology, 2022 **Abstract**: Dispersal is crucial in governing species response toward climate warming. Previous studies suggest that intermediate and density-dependent dispersal enables the functioning of a metacommunity, stabilizing populations at local and regional scales. Here, we consider a spatial ecological model with temperature-dependent traits to elucidate dispersal effects in stabilizing population dynamics under climate warming. Specifically, we analyze the effect of species temperature-dependent life-history traits on a metacommunity dynamics with diverse dispersal strategies (i.e., constant and density-dependent dispersal), tracked along with different dispersal rates of species (relative dispersal). At low and intermediate temperatures, different dispersal strategies synchronize or desynchronize the population dynamics depending upon dispersal rates. However, high temperatures completely synchronize the population trailing constant dispersal, weakening the stabilizing dynamics. Furthermore, density-dependent dispersal strongly affects the stability of metacommunity at high temperatures by increasing or decreasing spatial synchrony depending on dispersal rates. In metacommunities with many patches, conditional upon temperature, species abundance exhibits coexistence of synchronous and asynchronous oscillations, namely the chimera state. Overall, our results show that rising temperature may destabilize the dynamics by synchronizing populations; however, some dispersal mechanisms might impede the adverse outcomes.
18.	Clinical Characteristics and Treatment Outcomes of Mild to Moderate COVID-19 Patients at Tertiary Care Hospital, Al Baha, Saudi Arabia: A Single Centre Study M Albanghali, S Alghamdi, M Alzahrani, B Barakat… JA Malik - Journal of Infection and Public Health, 2022 **Abstract**: Objective Since the severity of symptoms affects the treatment option for Coronavirus Disease 2019 (COVID-19) patients, the treatment pattern for mild to moderate non-ICU cases must be

	evaluated, particularly in the current scenario of mutation and variant strain for effective decision making. Methods The objective of retrospective analysis was to assess clinical and treatment outcomes in mild to moderate symptoms in non-ICU patients with COVID-19 who were admitted to major tertiary care hospitals in Al Baha, Saudi Arabia, between April and August 2020. Results A total of 811 people were admitted for COVID-19 treatment, age ranging from 14 to 66, diabetes mellitus (31%, n = 248) and hypertension (24%, n = 198) were the most common comorbid conditions. The hydroxychloroquine (HCQ) treated group (G1 n = 466) had an MD of 8 and an IQR of 5-13 for time in hospital with a 4.3% mortality rate, while the non-HCQ group (G2 n = 345) had an MD of 6 and an IQR of 3-11 for time in hospital with a 3.2% mortality rate. A combination of antiviral and antibiotic treatment was found to be effective, other most frequent intervention was analgesics 85.7%, anticoagulant 75%, minerals (Zinc 83% and Vit D3 82%). Conclusions The therapy and clinical outcomes from the past will be the guiding factor to treat the COVID variants infection in the future. Patients treated with HCQ had a higher mortality rate, whereas those who were given a non-HCQ combination had a greater clinical outcome profile.
19.	Comparative Analysis of Outer Rotor Five Phase Switched Reluctance Motor with Higher Rotor Poles Configurations for EV Application Z Rayeen, S Payami - IEEE International Conference on Power Electronics, Smart Grid, and Renewable Energy, 2022 **Abstract**: This paper presents the design conditions and the performance of the outer rotor five-phase switched reluctance motor (OR-FPSRM) with a higher rotor pole configuration for Electric vehicles (EV) applications. The design considerations of pole arc angle selection, pole enclosure, and slot area for different rotor pole combinations have been discussed and their effect on the performance of the motor is investigated. OR-FPSRM with higher rotor pole configuration (10/8, 10/12, 10/14 & 10/16) of constant core volume has been designed by the above considerations and optimized by the genetic algorithm. The comparative analysis of various performance factors such as speed, torque, core losses, and copper losses for the OR-FPSRM and its higher rotor poles combination have been shown. The analysis of the motor has been carried out in the Ansys Maxwell environment.
20.	Comparative Evaluation of SiC based Two-Level Inverter With Passive EMI Filter Against Dual Two-Level Inverter Under PWM Schemes TJ Nistane, M Kumar, K Jayaraman - IEEE International Conference on Power Electronics, Smart Grid, and Renewable Energy, 2022 **Abstract**: The two-level (TL) inverter employs a passive EMI filter to mitigate conducted common-mode (CM) electromagnetic interference (EMI) issues such as CM current and shaft voltage. Whereas the topology of dual two-level (DTL) inverter is emerged with the provision of dedicated pulse width modulation (PWM) scheme to eliminate the CM voltage and thereby considers the reduction of CM emissions in the system. However, the effect of CM voltage elimination on the attenuation performance of high frequency CM noise (up to 30 MHz) and

	shaft voltage in DTL inverter fed induction motor is not clearly stated in literature. Thus, this paper presents the theoretical and experimental discussion on comparative evaluation between TL inverter system with passive EMI filter and the DTL inverter under PWM schemes such as CM voltage elimination (CMV E) PWM and remote state PWM (RSPWM) scheme. The comparative evaluation is carried out in terms of attenuation of conducted CM emissions in relevance to the component requirement for both the systems. The experimental verification of the reported work is carried out for a 3-ϕ, 1.1 kW IM driven in star configuration for TL inverter and open-end winding configuration for DTL inverter.
21.	Complexity of Paired Domination in AT-free and Planar Graphs V Tripathi, T Kloks, A Pandey, K Paul… - Conference on Algorithms and Discrete Applied Mathematics: Part of the Lecture Notes in Computer Science book series, 2022 **Abstract**: For a graph G=(V,E) , a subset D of vertex set V, is a dominating set of G if every vertex not in D is adjacent to atleast one vertex of D. A dominating set D of a graph G with no isolated vertices is called a paired dominating set (PD-set), if G[D], the subgraph induced by D in G has a perfect matching. The Min-PD problem requires to compute a PD-set of minimum cardinality. The decision version of the Min-PD problem remains NP-complete even when G belongs to restricted graph classes such as bipartite graphs, chordal graphs etc. On the positive side, the problem is efficiently solvable for many graph classes including intervals graphs, strongly chordal graphs, permutation graphs etc. In this paper, we study the complexity of the problem in AT-free graphs and planar graph. The class of AT-free graphs contains cocomparability graphs, permutation graphs, trapezoid graphs, and interval graphs as subclasses. We propose a polynomial-time algorithm to compute a minimum PD-set in AT-free graphs. In addition, we also present a linear-time 2-approximation algorithm for the problem in AT-free graphs. Further, we prove that the decision version of the problem is NP-complete for planar graphs, which answers an open question asked by Lin et al. (in Theor. Comput. Sci., 591(2015):99−105 and Algorithmica, 82(2020):2809−2840).
22.	Contact electrification through interfacial charge transfer: a mechanistic viewpoint on solid–liquid interfaces PK Panda, D Singh, MH Köhler, DD de Vargas, ZL Wang, R Ahuja - Nanoscale Advances, 2022 **Abstract**: Contact electrification (triboelectrification) has been a long-standing phenomenon for 2600 years. The scientific understanding of contact electrification (triboelectrification) remains un-unified as the term itself implies complex phenomena involving mechanical contact/sliding of two materials involving many physico-chemical processes. Recent experimental evidence suggests that electron transfer occurs in contact electrification between solids and liquids besides the traditional belief of ion adsorption. Here, we have illustrated the Density Functional Theory (DFT) formalism based on a first-principles theory coupled with temperature-dependent ab initio molecular dynamics to describe the phenomenon of interfacial charge transfer. The model captures charge transfer dynamics upon adsorption of different ions and molecules on AlN (001), GaN (001), and Si (001) surfaces, which reveals the influence of interfacial charge transfer and can predict charge transfer differences between materials. We have depicted the substantial difference in charge transfer between fluids and solids when different ions (ions that contribute to physiological pH variations in aqueous solutions, e.g., HCl for acidic pH, and NaOH for alkaline pH) are adsorbed on the surfaces. Moreover, a clear picture has been provided based on the electron localization function as conclusive evidence of contact electrification, which may shed light on solid–liquid interfaces.

23.	Contribution of typhoid toxin in the pathogenesis of Salmonella Typhi R Thakur, CR Suri, P Rishi - Microbial Pathogenesis, 2022 **Abstract**: To persist and establish infection, Salmonella utilizes a battery of different virulence determinants at every stage of infection. Typhoid toxin, a newly identified toxin in Salmonella enterica serovar Typhi is recognized as one of the virulence factors that has been linked with Salmonella pathogenesis. In this study, we have further investigated the role of typhoid toxin in the symptomatology of typhoid fever through in-vivo and ex-vivo studies. In mice, administration of cloned and purified typhoid toxin induces similar symptoms observed during typhoid fever such as fever, weight loss with a decrease in peripheral leucocyte count along with an increase in levels of pro-inflammatory cytokines (Il-6, TNF-α). Results of DNA analysis, fluorescence microscopy and flow cytometry of typhoid toxin-treated macrophages (ex-vivo) altogether revealed the CdtB (subunit of typhoid toxin) mediated DNA damage that led to the apoptosis of cells. Furthermore, to validate CdtB's catalytic role, macrophages were treated with typhoid toxin preincubated with anti-CdtB antibodies (generated in mice). Re-assessment of macrophage DNA by gel electrophoresis and flow cytometry analysis indicated a significant decrease in DNA damage and cells undergoing apoptosis, respectively. Moreover, a significant reduction in in-vitro DNase activity of CdtB protein was also observed on preincubating holotoxin with anti-CdtB antibodies. In total, this study highlights the role of typhoid toxin in inducing typhoid fever-like symptomatology, which may be executed through the toxin's catalytic subunit CdtB.
24.	Crystallinity modulation originates ferroelectricity like nature in piezoelectric selenium NR Alluri, NPMJ Raj, G Khandelwal, PK Panda…R Ahuja… - Nano Energy, 2022 **Abstract**: Modern room temperature ferroelectrics/piezoelectrics significantly impact advanced nanoelectronics than conventional chemical compounds. Changes in crystallinity modulation, long-range order of atoms in metalloids permits the design of novel materials. The ferroelectric like nature of a single element (selenium, Se) is demonstrated via in-plane ($E\perp^{ar}$ to the Se helical chains in micro-rod (MR)) and out-of-plane ($E \parallel^{el}$ to the Se helical chains in MR) polarization. Atomic electron microscopy shows large stacks of covalently bound Se atoms in a c-axis orientation for tip bias voltage-dependent switchable domains with a 180° phase and butterfly displacement curves. The single crystalline Se MR has a high in-plane piezoelectric coefficient of 30 pm/V relative to polycrystalline samples due to larger grains, crystal imperfections in MR, and tuned helical chains. The energy conversion of a single Se-MR demonstrated via d_{13}, d_{12} (or d_{15}) piezoelectric modes.
25.	Delineating Flood Zones upon Employing Synthetic Aperture Data for the 2020 Flood in Bangladesh M Aziz, M Moniruzzaman, A Tripathi, M Hossain… - Earth Systems and Environment, 2022 **Abstract**: Delineating a flood map is critical to perceive the potential risks of the event at diverse communities living both in urban and rural settings in Bangladesh. A timely generated flood map can help determine the losses of properties, calculate payment options from insurances, and set up mitigation measures when required. Application of satellite remote sensing (RS) and geographic information systems (GIS) are common these days to determine inundated areas, and to calculate possible losses of economies at scale. However, challenges remain while considering the available options for collecting satellite imageries obtained during the monsoon season with more than 70% cloud coverages found in the data. As a result, active synthetic aperture radar (SAR) sensors are a better choice to utilize the data in delineating the inundated areas. In doing

	so, this scientific paper sets up a few objectives to (1) prepare a flood map of Bangladesh using SAR remote-sensing data available from Sentinel-1 satellite; and (2) generate the inundated maps using cloud-based product, i.e., Google Earth Engine (GEE) in categorizing flood-affected districts of Bangladesh in 2020. Results have demonstrated that approximately 11% area of Bangladesh has been affected by the 2020 flood mainly located in the north-central and north-eastern part of the country. Moreover, the old Brahmaputra floodplain, Tista floodplain, lower Ganges-River floodplain, and Karataya-Bangali floodplain have been severely affected by the flood. Note that, the GEE-based automated processing systems adopted in this study have enhanced the computational time while obtaining freely available satellite data to generate mitigation strategies for the betterment of the communities suffered by the flood event.
26.	Design of noble metal-free $NiTiO_3/ZnIn_2S_4$ heterojunction photocatalyst for efficient visible-light-assisted production of H_2 and selective synthesis of 2,5-Bis(hydroxymethyl)furan S Dhingra, M Sharma, V Krishnan, CM Nagaraja - Journal of Colloid and Interface Science, 2022 **Abstract**: In this work, the development of noble metal-free $NiTiO_3/ZnIn_2S_4$ (1:0.25 (S1), 1:0.5 (S2), 1:1 (S3), and 1:2 (S4)) heterojunction photocatalysts possessing optimal band edge positions suitable for efficient production of H_2 from water and in situ reduction of biomass derivative, 5-hydroxymethylfurfural (HMF) to value-added 2,5-Bis(hydroxymethyl)furan (BHMF) in the absence of any external reducing agent is presented. The electron microscopy analysis of these heterojunctions revealed that $ZnIn_2S_4$ nanosheets are decorated uniformly over the surface of NiTiO3 microrods. Interestingly, heterojunction, S3 having $NiTiO_3/ZnIn_2S_4$ (1:1) showed the best photocatalytic activity with a high H2 generation rate of 4.43 mmol g−1h−1 which is about eight times higher than that of pure $ZnIn_2S_4$. Further, the photocatalytic H2 evolution activity of S3 was coupled with in situ reduction of biomass derivative, HMF to obtain value-added chemical, BHMF with > 99% yield along with 100% selectivity. This high photocatalytic activity of S3 is aided by the Z-scheme heterojunction between $NiTiO_3$ and $ZnIn_2S_4$. Moreover, photocatalyst, S3, showed excellent photostability and retained the catalytic activity for several cycles of reuse. Overall, this work represents a unique demonstration of H2 generation and high yield production of an important commodity chemical, BHMF from biomass-derivative and provides a greener path for harvesting solar energy and its conversion to chemical energy.
27.	Diosmin, a citrus fruit-derived phlebotonic bioflavonoid protects rats from chronic kidney disease-induced loss of bone mass and strength without deteriorating renal function S Sharma, K Porwal, C Kulkarni, S Pal, P Sihota, S Kumar…N Kumar… - Food & Function, 2022 **Abstract**: Kidney Disease Improving Global Outcomes (KDIGO) 2017 Clinical Practice Guideline has recommended treatment decisions for patients with chronic kidney disease (CKD) with osteoporosis and/or high risk of fracture. Bisphosphonates, the first-line anti-osteoporosis drugs have the concern of worsening kidney functions. Moreover, despite impaired bone formation in CKD patients, teriparatide, the formation-stimulating drug is not recommended. Thus, there is an urgent need for safe and effective treatment of osteoporosis in CKD patients. Here, in CKD rats, we tested the osteoprotective effect of diosmin, a citrus-derived bioflavonoid used as a phlebotonic in chronic venous insufficiency and has a renoprotective effect. CKD was developed by 5/6th nephrectomy and diosmin at the human equivalent dose (100 mg kg−1) did not advance renal failure but reduced blood pressure to the level of sham control. Fibroblast growth factor-23 and parathyroid hormone were increased in CKD and diosmin suppressed both.

	CKD reduced bone mass and deteriorated the microarchitecture of trabecular bones, and diosmin maintained both to control levels. Bone formation and strength were impaired in the CKD and diosmin maintained these levels to control levels. Nanoindentation of bone showed that diosmin significantly increased tissue hardness over the control. Diosmetin, the metabolic surrogate of diosmin had comparable pharmacokinetic profiles between the control and CKD groups. Furthermore, diosmetin (50 mg kg−1) protected against CKD-induced bone loss. These data suggest that diosmin and its metabolic surrogate, diosmetin protect against CKD-induced osteopenia. Since diosmin has no renal adverse effect and protected bone mass and strength in CKD rats, we propose assessing its anti-osteoporosis effect in CKD patients.
28.	Dual-Purpose Planar Radial-Array of Rectenna Sensors for Orientation Estimation and RF-Energy Harvesting at IoT Nodes M Kumar, S Kumar, A Sharma - IEEE Microwave and Wireless Components Letters, 2022 **Abstract**: A dual-purpose radial-array rectenna is presented as a potential sensor candidate for RF-energy harvesting (EH)-enabled Internet of Things (IoT) nodes along with orientation sensing capability. The proposed design comprises eight rectenna elements placed radially in azimuth to capture RF energy from entire 360° angular region to improve tolerance for angular misalignment and make the design orientation-oblivious. As dual-purpose, the capability to sense its own orientation with respect to the transmitter is additionally provided. Each rectenna consists of a horizontally polarized compact planar scoop-shaped antenna designed at 5.8 GHz having endfire radiation pattern with 7-dBi gain. The dc power patterns of the proposed design are calibrated and used to estimate orientation using minimum mean square error (MMSE) method. The design is verified experimentally, and the results indicate average orientation estimation error of 1.0822° with 0.9242° standard deviation and improved stability in energy-harvesting compared to single rectenna element for varying orientation of IoT nodes.
29.	Effect of projectile structure on break-up fusion for ^{14}N+ ^{175}Lu system at intermediate energies IM Bhat, M Shuaib, MS Asnain, VR Sharma, A Yadav…PP Singh… - Nuclear Physics A, 2022 **Abstract**: In the present work, fusion in heavy-ion collisions at energies near the Coulomb barrier to ≈ 33% above it has been studied for ^{14}N + ^{175}Lu system. The excitation functions of several reaction channels expected to be populated via complete fusion and/or the incomplete fusion of the projectile have been measured. The experimental excitation functions have been critically compared with the predictions of the statistical model code PACE4. The observed enhancement in the measured cross-sections with respect to the theoretical model code PACE4 predictions of all the reactions having α-particle(s) in the exit channel is reminiscent of the fact that incomplete fusion (ICF) is at work in populating these channels besides the complete fusion process. The relative probability of incomplete fusion in fusion dynamics, obtained in terms of incomplete fusion strength function FICF has also been deduced. The observed behavior of FICF suggests the increasing probability of ICF contributions with projectile energy. A strong and a dictating dependence of FICF on projectile structure in terms of its Qα-value has been observed. The reduction procedures for the elimination of the geometric and the static effects suggest that the observed variation in the fusion data has a purely static origin i.e., a manifestation of different potential barriers and radii. The analysis done within the framework of universal fusion function indicates the fusion suppression of ≈ 5% for the ^{14}N + ^{175}Lu system.
30.	Effect of Ripple in DC on Voltage Endurance Coefficient of Cable Insulation Based on Damage Equalization Method BS Thind, CC Reddy - IEEE Conference on Electrical Insulation and Dielectric Phenomena, 2021

	Abstract: In the offshore transmission systems, the converters are used for AC to DC and DC to AC conversion. The utilization of HVDC cable transmission over AC transmission in offshore wind farms is quite efficient. On the DC side, the polymeric insulated cables are stressed by the DC voltage with huge amount of ripple content. The accelerated aging tests were performed to confirm the effect of the ripple voltage on the degradation of the cable insulation. The breakdown tests were performed on LDPE samples using ripple voltage with frequency of 500 Hz superimposed on DC voltage. This work investigates the effect of ripple voltage on the life of the offshore HVDC cable, that it is always important to consider interactions of all the system components while designing the cable insulation.
31.	Effects of noise correlation and imperfect data sampling on indicators of critical slowing down T Kaur, PS Dutta - Theoretical Ecology, 2022 **Abstract**: Critical slowing down-based early warning signals (EWSs) are well-known indicators that precede an approaching collapse in complex systems. To date, the majority of studies on the predictability of critical transitions consider systems perturbed with temporally uncorrelated noise. In contrast, here we study catastrophic and non-catastrophic transitions, and the performance of associated EWSs in systems perturbed with correlated noise. We find that elevated noise correlation can advance the occurrence of a catastrophic transition, and simultaneously progresses the system's recovery. However, noise correlation does not have a significant impact on the likelihood of non-catastrophic transitions. We show that depending upon the transition mechanism, the occurrence of weak to false signals increases with noise reddening. Imperfect data sampling, both spatial and temporal, further reduces the efficacy of EWSs. Spatially limited data has more impact on the efficacy of EWSs for negative noise correlation than that of positive. However, temporally imperfect data is more detrimental for positively correlated noise. Overall, our study suggests that performance of EWSs is critical to system-specific perturbations as well as data sampling.
32.	Efficient production of hydrogen from H_2S via electrolysis using a $CoFeS_2$ catalyst M Kumar, TC Nagaiah - Journal of Materials Chemistry A, 2022 **Abstract**: Transformation of noxious and undesirable industrial waste H_2S into hydrogen (H_2) *via* electrolysis will be a game-changing strategy. Herein, we have developed a cost-effective and highly stable nanorod embedded wheat grain $CoFeS_2$ in conjugation with a nitrogen containing carbon framework for pure H_2 production from H_2S by reduction at the cathode and the sulfide oxidation reaction (SOR) at the anode. The proposed catalyst exhibits the lowest onset potential of 0.23 V *vs.* RHE to drive H_2S electrolysis which is 1.0 V lower than the thermodynamic potential of electrochemical water splitting (1.23 V). Moreover, it demonstrates 97.8% H_2 faradaic efficiency with remarkable durability up to 120 h. These outcomes demonstrate a promising future prospective of H_2S as a cost-effective H_2 source towards a more sustainable economy simultaneously eliminating the environmental pollutant.
33.	Electrical Distribution System Fault Location Using Soft Clustering Mean and Statistical Method P Arvind, S Murala, A Verma, J Kumar, RP Maheshwari - Recent Advances in Power Systems: Part of the Lecture Notes in Electrical Engineering book series, 2022 **Abstract**: Electrical power distribution network is an integral part of electrical power systems since it is the last stage in the delivery of electricity to customers. The distribution network is responsible for distributing power to consumers at desired voltage levels with higher reliability. Alternating Current (AC) three phase four-wire structure is the standard distribution system that

	exists throughout the world. With the growth in urban population and development of industries, distribution grids now consider a considerable amount of power. The large number of lines in a distribution system experience regular faults which lead to high values of line currents. In the present work, an alternate solution to the problems related with interruptions by means of a statistical modeling of current sample database is applied to determine the fault location in power distribution systems in order to reduce the system restoration time. The current samples collected from the sample distribution systems are subjected to FCM to obtain clusters and fed to expectation–maximization algorithm. It gives an edge over the conventional impedance-based methods and also the problem of multi estimation has been successfully dealt.
34.	Electro-thermal Dynamics During Load Cycle and Polarity Reversal of HVDC Cables Under Different Soil Conditions S Dhayalan, AH Kumar, P Johri, CC Reddy - International Conference on Electrical, Computer and Energy Technologies, 2021 **Abstract**: The advent of polymeric cables is believed to be one of the greatest breakthroughs in the field of HVDC power transmission. With time, various problems associated with the polymeric cables came into light. This led to an increased interest in the investigation of the effect of transients rather than the much-explored steady state behavior. In the current work, the authors present a design performance analysis of a HVDC cable exploring the effect of soil surrounding the cable on the electro-thermal stresses experienced by the insulation. The cable has been simulated for different soil thermal properties, under Cigre standard TB 496 based load cycle with polarity reversal, to get a better understanding of the effect of the geographical location of installation of the cable.
35.	Energy-Aware Trajectory Design for Outage Minimization in UAV-Assisted Communication Systems N Gupta, D Mishra, S Agarwal - IEEE Transactions on Green Communications and Networking, 2022 **Abstract**: This paper studies the flight trajectory of unmanned aerial vehicles (UAV) to provide fifth-generation (5G) cellular service in a given area. We consider a single UAV launched from the fixed initial to the final location, during which it serves the ground users that are distributed in a circular field. UAV's limited on-board energy has been a major concern affecting the system's performance. Therefore, in this work, we minimize the average outage probability of the system by optimizing the three-dimensional (3D) trajectory of the UAV while considering the velocity and on-board energy as constraints. To solve this problem, we propose two approaches: the low-complexity vertex and the high-performance sequential approach. The vertex approach involves two steps. Firstly, it obtains the optimal solution while relaxing the velocity and on-board energy constraints. Secondly, a greedy solution is proposed for the original problem. The sequential approach finds the optimal location in each time slot sequentially. Simulation results compare the two approaches and show that our proposed strategies provide on an average 41% improvement in average outage probability over the benchmark schemes. Additionally, we show that the sequential approach is better than the vertex approach, though at the cost of high computational complexity.
36.	Engineered Polymeric Materials/Nanomaterials for Growth Factor/Drug Delivery in Bone Tissue Engineering Applications N Chauhan, Y Singh - Nanoscale Engineering of Biomaterials: Properties and Applications, 2022

	Abstract: Accelerating number of bone fractures/disorders, increased global burden, high demand, and limited availability of traditional bone grafts have shifted the research interest toward development of alternatives strategies, including the development of growth factor/drug delivery systems. The conventional delivery methods are limited in application due to the poor local retention, half-life, stability, requirement of high dosage, and inactivation of growth factor and drugs in biological systems. Polymeric materials/nanomaterials have emerged as promising candidates for therapeutic delivery of growth factors and drugs in tissue engineering applications due to their functionality and highly porous structure, which is suitable for high drug loading and extracellular-mimicking properties that promote cell attachment and proliferation for tissue repair. Engineering of polymeric materials has resulted in advancement of polymer chemistry in drug delivery applications by providing stimuli-sensitive polymeric systems, which can respond to pH, temperatures, and the presence of biomolecules. Different polymeric structures, such as nanofibers, nanoparticles, hydrogels, and 3D-printed scaffolds, have been investigated to overcome the problem of low drug efficacy and burst release. The polymeric materials maximize the effectiveness of growth factors/drugs by providing sustained, controlled, and localized release. However, the selection of polymers and growth factors/drugs is significantly important for the optimization and development of drug release systems similar to the release of growth/osteogenic factors in natural bone healing. This chapter focuses on the design strategies being employed for the next-generation engineered polymeric material/nanomaterial-based advanced delivery systems for enhancing the bone repair and regeneration as well as their potential application in regenerative medicine.
37.	Enhancement of collection efficiency for capturing submicron particles emitted from biomass burning: a novel design of semi-circular corrugated plate electrostatic precipitator A Varshney, NK Mishra, R Das - Biomass Conversion and Biorefinery, 2022 **Abstract**: This paper presents the study of a novel semi-circular corrugated wire-plate electrostatic precipitator (ESP) for capturing submicron particles emitted from the burning of biomass residue. The discharge of residual gases from biomass combustion is widely acknowledged to be hazardous to human health. The main objective of ESP is to control the release of residual gases. The numerical simulation was performed to evaluate the collection efficiency, space charge density, electric field, gas dynamics, and flow behaviour in the ESP with flat and semi-circular corrugated plates. The influence of electrohydrodynamic (EHD) flow and flow velocity on collection efficiency and particle trajectory had also been investigated at different applied voltages with various gas velocities. The results showed that the flow velocity had a significant influence on ESP performance and vortices formed in the flat plate ESP could be suppressed using a semi-circular corrugated plate ESP, which would be beneficial for collecting particles efficiently. The numerical results showed that the collection efficiency of semi-circular corrugated plate ESP compared to flat plate ESP is 33.33% higher for 2 μm and 25% for 5 μm particles.
38.	Evaluation of the Effectiveness of Base Insulation on the Productivity of a Packed Bed Solar Air Heater S Verma, R Das - Journal of Thermal Science and Engineering Applications, 2022 **Abstract**: Effect of bottom surface thermal energy loss for a packed bed solar air heater is investigated using both one dimensional transient as well as steady state models. While the former is solved numerically, closed form solution is obtained for the latter. Effect of variation in base insulation thickness on the system output is studied. For a given bottom insulation thickness, dependence of its effectiveness on various thermo-geometric parameters is also

	analyzed. It is observed that a collector with an uninsulated base loses about 60 % of the available incident solar energy. In comparison, when the base insulation is as thick as the base wall, i.e., 50 mm here, the base loss fraction drops to nearly 6 %, thus, highlighting the importance of base insulation. Further, it is seen that the efficiency of a particular base insulation thickness lessens with larger length and width of collector, and rises with larger mass flow rate of air flowing through it. This work presents a mathematical tool to calculate appropriate insulation thermal resistance to be applied at the base of packed bed solar air heaters that yields best possible thermal performance alongside minimum insulation cost.
39.	Experimental investigation on magnesium AZ31B alloy during ultrasonic vibration assisted turning process N Deswal, R Kant - Materials and Manufacturing Processes, 2022 **Abstract**: Magnesium alloys generate harmful emissions while using coolants during the machining process and it affects both the operator and the environment. Ultrasonic vibration assisted turning (UVAT) is an eco-friendly and advanced machining process to machine various materials than conventional turning (CT). In this study, experimental analysis is carried out to investigate the machinability of the magnesium AZ31B alloy during CT and UVAT processes. The effect of cutting speed during the processing of magnesium AZ31B alloy is analyzed and compared with CT in terms of machining forces, machining temperature, tool wear, chip morphology, surface roughness, microstructure, and microhardness. Results showed that compared with CT, machining forces and surface roughness is reduced significantly in UVAT. However, higher machining temperature is obtained during UVAT than CT. Flank wear is observed during CT although negligible tool wear is observed for UVAT. Chip segmentation is obtained for both CT and UVAT whereas higher chip thickness is observed for UVAT than CT process. Finer grains and higher microhardness are obtained in UVAT than the coarse grains and lower microhardness in CT. The results showed that the processing of magnesium AZ31B alloy during the UVAT process leads to enhanced machining performance compared to the CT process.
40.	Experimental study of fast fission and quasifission in the ^{40}Ca + ^{208}Pb reaction leading to the formation of the transfermium nucleus ^{248}No EM Kozulin, GN Knyazheva, AA Bogachev, VV Saiko…PP Singh - Physical Review C, 2022 **Abstract**: **Background:** The stability of the transfermium nucleus against fission is mainly determined by the shell correction depending on its angular momentum and excitation energy. **Purpose:** The study of the fast fission process of the transfermium nucleus ^{248}No and its dependence on the interaction energy and introduced angular momentum. **Methods:** Mass-energy distributions of the ^{248}No fission fragments formed in the ^{40}Ca + ^{208}Pb reaction at energies above the Coulomb barrier have been measured using the double-arm time-of-flight spectrometer CORSET at the ^{40}Ca-beam energies of 223, 250, and 284 MeV. **Results:** The contribution of the fast fission process is determined from the calculations of the driving potential, taking into account shell effects and rotational energy and amounts to 39% and 61% at 250 and 284 MeV, respectively. The mass-energy distributions of the quasifission and fast fission fragments have been extracted by subtracting the mass-energy matrices associated

	with compound nucleus fission from those of all measured fissionlike events. The asymmetric fragments with masses 97 and 151 u were found to be the most probable in the fast fission of ^{248}No. With increasing ^{40}Ca energy from 250 to 284 MeV the mass distributions of the fast fission fragments change slightly. **Conclusions:** Contrary to quasifission in which the fragments are focused mainly around the closed neutron or proton shells, the influence of known proton or neutron shells on the asymmetric mass distribution in the fast fission process was not observed.
41.	Face Verification System with Liveness Detection D Srivastava, P Shukla, AK Sahani - IEEE 18th India Council International Conference, 2021 **Abstract**: Many developments have taken place in the field of face-recognition and liveness analysis to improvise various device securities and attendance verification systems. Many approaches have incorporated 3D analysis of the face to predict the liveness of the person in front of it. Our method tries to account for this problem without using advanced 3D imaging techniques or hardware. This results in a solution that is both, more economical and also much easier to deploy. It consists of two parts; the former helps in face verification and the latter to check the liveness of the face. In the first part, we have used a model based on Google's FaceNet Model which learns a mapping from face images to compact Euclidean space distances, which directly correspond to the measure of similarity of the images. Once the space has been produced, face verification can be easily implemented using standard techniques with embeddings as feature vectors. For the second part, we have employed a cascaded multi-task framework that extracts certain features from the facial image which are then used to check for liveness by tracking their relative displacements. These extracted features were used to check the liveness of the person's face by asking them to perform some tasks in a random order like head and facial movements etc.
42.	Fast Discharging (N+1) Switch Converter with Regenerative Flyback Operation for N-phase SRM Drives AK Rana, AVR Teja - IEEE Transactions on Power Electronics, 2022 **Abstract**: This paper proposes a converter topology that can provide fast discharging for any N-phase SRM drive. The proposed converter achieves fast discharging with only (N+1) switches for an N-phase SRM drive. The discharging can also be varied and made faster as per requirement. The proposed converter achieves fast discharging by dumping the winding energy to a capacitor and feeding it back to the source through a flyback transformer. The proposed converter uses fewer switches, is easy to control, and has variable discharging voltage which can be made much greater than the supply voltage. The proposed converter has been implemented with a 4-phase SRM drive using MATLAB/Simulink software and the results are presented. A hardware prototype of the proposed converter is developed in the laboratory and tested on a 4-phase SRM. The corresponding experimental results are presented at different operating conditions. The proposed converter is also compared with other existing SRM converters with respect to different performance metrics and a detailed comparison table is presented. Using the proposed converter, a minimum discharge time of 0.32 ms has been achieved at 3 A reference current.
43.	Fission of ^{182,183}Hg Nuclei at Energies Around the Coloumb Barrier M Cheralu, YS Mukhamejanov, EM Kozulin…PP Singh… - Acta Physica Polonica B Proceedings Supplement, 2021

	Abstract: Asymmetric fission of mercury nuclei was initially observed in the lowenergy region. In recent years, several experiments have been performed in this direction to investigate the asymmetric behaviour of Hg nuclei which supported the influence of shell effects on the asymmetric fission process. An experiment was performed using the CORSET setup. We investigated mass and energy distributions of fragments and fission characteristics of prolately-deformed ^{182}Hg and oblately-deformed ^{183}Hg nuclei formed in the ^{40}Ca+^{142,143}Nd reactions at three different beam energies — E_{lab} = 172, 192, and 212 MeV. We found no huge variation in mass–energy distributions of ^{182}Hg and ^{183}Hg at any of the measured energies. This gives us an outlook regarding the influence of shell structure, charge radii deformation, and factors associated with the potential energy surface that is responsible for fission in the Hg region.
44.	Full Duplex Relay Assisted Coded Cooperation for Next Generation Wireless Networks S Bhattacharyya, P Kumar, S Darshi, O Burnwal… - IEEE 18th India Council International Conference, 2021 **Abstract**: Wireless networks based on Network Coded Co-operation (NCC) have shown promising results in achieving faster and reliable communication. To make the next-generation wireless systems swifter, the nodes can be equipped to work in Full-Duplex (FD) mode. In this paper, we thus model a multi source-destination NCC scenario with a relay working in FD mode (FD-NCC) and propose a decoding scheme for it. FD schemes have the benefit of an increased achievable rate. Extensive simulations carried out in MATLAB show an improved performance for FD in terms of achievable rate when compared to a Half-Duplex NCC (HD-NCC) scenario. NCC systems aided by a FD relay, also provides higher throughput thus, making it suitable for applications requiring reliable low latency communication (RLLC) in 5G/6G scenarios.
45.	Furfural–a versatile, biomass-derived platform chemical for the production of renewable chemicals A Jaswal, PP Singh, T Mondal - Green Chemistry, 2022 **Abstract**: For years, fossil fuels have been the predominant feedstock for the production of chemicals, resulting in their overexploitation and widespread environmental degradation, prompting a search for alternative feedstocks. In this context, lignocellulosic biomass has emerged as a green and inexhaustible carbon reservoir for the production of chemicals. Among the infinitely large number of chemicals that can be obtained from biomass is furfural, a commodity chemical with an annual production volume of nearly 652 kilotons. It has been recognised as one of the most valuable biomass-derived chemicals due to its high reactivity which allows it to serve as a platform compound for the synthesis of value-added chemicals. This review seeks to discuss both the processes for furfural production as well as its conversion to the most relevant chemicals, with greater focus on the latter part. Emphasis has been laid on providing a deep insight into the reaction conditions, systems and mechanisms involved in the transformation processes. Additionally, an effort has been made to highlight major challenges in the routes, suggest remedial solutions to them and discuss avenues for future work.
46.	High-capacity reversible hydrogen storage properties of metal-decorated nitrogenated holey graphenes E Anikina, SR Naqvi, H Bae, H Lee, W Luo, R Ahuja, T Hussain - International Journal of Hydrogen Energy, 2022 **Abstract**: Motivated by the need for an effective way of storing hydrogen (H2), a promising energy carrier, we have performed density functional theory (DFT) calculations with different van der Waals corrections coupled with the statistical thermodynamic analysis and ab initio

	molecular dynamics (AIMD) on the light-metal decorated nitrogenated holey graphene (C2N) monolayers. We have found that the decoration by selected light metals (Na, Mg, Ca) improves the H2 adsorption on the C2N to the desired levels (>150 meV/H2). Moreover, the metal dopants strongly bonded with C2N even at higher doping concentrations, which invalidates the metal clusters formation. Among considered metals, Na and Mg resulted in H2 storage capacities of 5.5 and 6.9 wt%, respectively, which exceed the target set by the U.S. Department of Energy's for 2025. Thermodynamic analysis and the AIMD simulations were employed to investigate the H2 sorption at varied conditions of temperature and pressure for practical applications. 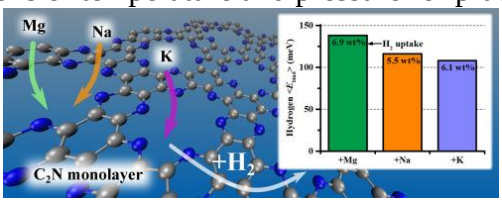
47.	High-performance computation of pricing two-asset American options under the Merton jump-diffusion model on a GPU A Ghosh, C Mishra - Computers & Mathematics with Applications, 2022 **Abstract**: This paper is concerned with fast, parallel and numerically accurate pricing of two-asset American options under the Merton jump-diffusion model, which gives rise to a two-dimensional partial integro-differential complementarity problem (PIDCP) with a nonlocal two-dimensional integral term. Following method-of-lines approach, the solution to the PIDCP can be computed quite accurately by a robust numerical technique that combines Ikonen–Toivanen splitting with an alternating direction implicit scheme. However, we observed that computing the numerical solution with this technique becomes extremely time consuming, mainly due to the handling of the integral term. In this paper we parallelize this technique by applying a parallel fast Fourier transformation algorithm to all matrix-vector multiplications involving the huge and dense integral approximation matrix by exploiting its block Toeplitz with Toeplitz block structure. We also parallelize other computationally intensive steps of this technique by applying a recently developed parallel cyclic reduction algorithm for pentadiagonal systems. Our solutions computed on a graphics processing unit (GPU) using CUDA® platform are compared for accuracy with those available in the literature. It is observed that by solving the PIDCP parallelly we could bring down the computational times from several hours to a few seconds in certain cases in our experiments.
48.	Impact of PWM and Duty Ratio Control on Voltage for Sic Fed Three Phase BLDC Motor Drive D Dwivedi, S Singh, J Kalaiselvi - IEEE International Conference on Power Electronics, Smart Grid, and Renewable Energy, 2022 **Abstract**: This paper presents an analysis of phase voltage and dc bus utilization for a three-phase Brushless DC motor (BLDC). Both pulse-amplitude (PAM) and pulse-width modulation (PWM) is employed to control the phase voltage and line current by adjusting the duty cycle. In this paper an analytical expression is derived for six-step-commutation, Bipolar PWM, HPWM-L-ON, and PWM-ON. Through analytical expression and experimentation a comparative analysis has been performed for the aforementioned PWM techniques. Experimental results on a three-phase star-connected Sic-based BLDC drive are provided to substantiate the analysis on phase voltage, and DC bus utilization.
49.	Improving Reliability of Transformers based on DGA Analysis using Machine Learning Techniques

	AH Kumar, BS Thind, CC Reddy - IEEE Conference on Electrical Insulation and Dielectric Phenomena, 2021 **Abstract**: Classifiers, Artificial Neural Networks (ANN), Fuzzy Logic (FL) and Adaptive Neuro Fuzzy Inference System (ANFIS) have been used as methods to detect faults using data obtained from Dissolved Gas Analysis (DGA). DGA provides reasonably good results in detecting insipient faults but improvement on the method's accuracy has been done. Comparative analysis using the mentioned methods have been done on IEC 599 standard, Rogers Ratio Method and Doernenburg's method. Fault databases have been used to train the models to improve the diagnostic capability. ANFIS has shown superiority on Classifiers, ANN and FL which is evident from the obtained results. ANFIS being a union of all the said methods, it has a higher prediction accuracy and is user friendly thereby, providing a promising surrogate in reinstating the conventional methods.
50.	Influence of artificial roughness parametric variation on thermal performance of solar thermal collector: An experimental study, response surface analysis and ANN modelling R Kumar, R Nadda, S Kumar, A Razak… - Sustainable Energy Technologies and Assessments, 2022 **Abstract**: The influence of the attack angle (α_a) of the perforated baffles on thermohydraulic performance ηp of a solar thermal collector (STC) has been investigated experimentally. The experimentations have been performed to obtain the Nusselt number (Nurs) and friction factor (f_{rs}) by varying Reynolds number (Re) from 5000 to 17,000 and αa from 35° to 65°. The other geometrical parameters of angled perforated baffles are fixed in accordance with previous studies. The relative baffle height HB/HD , relative baffle pitch PB/HB , relative hole position OB/HB and open area ratio β0 are fixed at 0.50, 10, 0.266 and 12% respectively. The STC with roughened angled perforated baffles improves the Nurs and f_{rs} by 3.82 and 7.14 times respectively as compared to STC without baffles wall. The angled perforated baffles at αa of 55° provides highest thermo-hydraulic performance at *Re* of 9000. A thermo-hydraulic performance of 1.94 is obtained for the array of designed parameters. The statistical correlations are established for the Nurs and frs by using experimental data. The correlations obtained for the Nurs and frs predict the experimental results within a variation of ±9.7% and ±5.0% respectively. Central Composite Design (CCD) of thermo-hydraulic performance parameters is carried for the surface response analysis. Modelling of thermal parameters using CCD and Artificial Neural Network (ANN) is done which predict them with good accuracy. The previously studies on STC roughened with various types of roughness show appreciable heat transfer enhancement but very few studies have utilized angled perforated baffles. As per author knowledge, a comprehensive study on the performance analysis of STC roughened with angled perforated baffles using different techniques is not available. The study become novel because in addition to the experimental examination of STC performance, correlations for Nurs and frs from experimental data are developed and modelling of thermal parameters using CCD and Artificial Neural Network (ANN) is also performed.
51.	Investigations on DC Breakdown in Solids under Needle tip-Plane Electrode Configuration AJ Thomas, CC Reddy - IEEE Conference on Electrical Insulation and Dielectric Phenomena, 2021 **Abstract**: Electrical treeing is considered to be one of the most important physical evidence of insulation damage in HV cables, caused due to the high field enhancement at the tip of these defects in the insulation. In this paper, breakdown experiments are conducted using needle-tip

	electrode configuration under stepped DC stress profile. Further, the authors present an estimation of electric field and space charge distributions in needle tip-plane system based on FEM. Nonlinear conduction is incorporated in the computation by using a semi-empirical equation of field and temperature-dependent conductivity. The results show the interesting aspects of nonlinear conductivity on the electric field and space charge distribution. Further, the effect of temperature dependence on field distribution at the needle-tip is also presented. Furthermore, from the breakdown experiments, the electric field at the tip is estimated for different tip radii and the results give a reasonable and realistic estimate of breakdown tip-field, using the proposed model.
52.	Ion transport and current rectification in a charged conical nanopore filled with viscoelastic fluids M Trivedi, N Nirmalkar - Scientific Reports, 2022 **Abstract**: The ionic current rectification (ICR) is a non-linear current-voltage response upon switching the polarity of the potential across nanopore which is similar to the I–V response in the semiconductor diode. The ICR phenomenon finds several potential applications in micro/nano-fluidics (e.g., Bio-sensors and Lab-on-Chip applications). From a biological application viewpoint, most biological fluids (e.g., blood, saliva, mucus, etc.) exhibit non-Newtonian visco-elastic behavior; their rheological properties differ from Newtonian fluids. Therefore, the resultant flow-field should show an additional dependence on the rheological material properties of viscoelastic fluids such as fluid relaxation time (λ) and fluid extensibility (ε). Despite numerous potential applications, the comprehensive investigation of the viscoelastic behavior of the fluid on ionic concentration profile and ICR phenomena has not been attempted. ICR phenomena occur when the length scale and Debye layer thickness approaches to the same order. Therefore, this work extensively investigates the effect of visco-elasticity on the flow and ionic mass transfer along with the ICR phenomena in a single conical nanopore. The Poisson–Nernst–Planck (P–N–P) model coupled with momentum equations have been solved for a wide range of conditions such as, Deborah number, $1 \le De \le 100$, Debye length parameter, $1 \le \kappa Rt \le 50$, fluid extensibility parameter, $0.05 \le \varepsilon \le 0.25$, applied electric potential, $-40 \le V \le 40$, and surface charge density $\sigma = -10$ and -50. Limited results for Newtonian fluid ($De = 0$, and $\varepsilon = 0$) have also been shown in order to demonstrate the effectiveness of non-Newtonian fluid behaviour over the Newtonian fluid behaviour. Four distinct novel characteristics of electro-osmotic flow (EOF) in a conical nanopore have been investigated here, namely (1) detailed structure of flow field and velocity distribution in viscoelastic fluids (2) influence of Deborah number and fluid extensibility parameter on ionic current rectification (ICR) (3) volumetric flow rate calculation as a function of Deborah number and fluid extensibility parameter (4) effect of viscoelastic parameters on concentration distribution of ions in the nanopore. At high applied voltage, both the extensibility parameter and Deborah number facilitate the ICR phenomena. In addition, the ICR phenomena are observed to be more pronounced at low values of κRt than the high values of κRt. This effect is due to the overlapping of the electric double layer at low values of κRt.
53.	Laser Micromachining in Fabrication of Reverse-μEDM Tools for Producing Arrayed Protrusions H Kishore, CK Nirala, A Agrawal - Micromachines, 2022 **Abstract**: This paper focuses on the fabrication of high-quality novel products using a μEDM process variant called Reverse-μEDM. The tool plate required for the Reverse-μEDM is fabricated using Nd: YAG-based laser beam micromachining (LBμM) at the optimized process parameters. The Grey relation analysis technique is used for optimizing LBμM parameters for

	producing tool plates with arrayed micro-holes in elliptical and droplet profiles. Titanium sheets of 0.5 mm thickness were used for such micro-holes, which can be used as a Reverse-µEDM tool. The duty cycle (a combination of pulse width and frequency) and current percentage are considered as significant input process parameters for the LBµM affecting the quality of the micro-holes. A duty cycle of 1.25% and a current of 20% were found to be an optimal setting for the fabrication of burr-free shallow striation micro-holes with a minimal dimensional error. Thereafter, analogous protrusions of high dimensional accuracy and minimum deterioration were produced by Reverse-µEDM using the LBµM fabricated tool plates.
54.	Learning Safe Cooperative Policies in Autonomous Multi-UAV Navigation A Singh, SS Jha - IEEE 18th India Council International Conference, 2021 **Abstract**: The deployment of multiple Unmanned Aerial Vehicles (UAV) in constrained environments has various challenges concerning trajectory optimization with the target(s) reachability and collisions. In this paper, we formulate multi-UAV navigation in constrained environments as a multi-agent learning problem. Further, we propose a reinforcement learning based Safe-MADDPG method to learn safe and cooperative multi-UAV navigation policies in a constrained environment. The safety constraints to handle inter-UAV collisions during navigation are modeled through action corrections of the learned autonomous navigation policies using an additional safety layer. We have implemented our proposed approach on the Webots Simulator and provided a detailed analysis of the proposed solution. The results demonstrate that the proposed Safe-MADDPG approach is effective in learning safe actions for multi-UAV navigation in constrained environments.
55.	Low-Voltage, self-powered and broadband photodetector with Ohmic, transparent and cost-effective AZO electrodes on vertical aligned MoS_2 flakes AV Agrawal, N Kumar, D Kumar, SK Jain, G Gupta…M Kumar - Surfaces and Interfaces, 2022 **Abstract**: The transparent Ohmic electrodes are the extreme necessity to develop cutting-edge broadband photodetectors. Conventional metal electrodes reflect incident light and diminish overall performance of photodetector. Here, we report cost-effective, transparent Ohmic Al-doped ZnO (AZO) electrodes to develop self-powered, highly responsive photodetectors from visible to near-infrared regions using vertically-aligned MoS_2 (VA- MoS_2) flakes. The MoS_2 photodetector with AZO electrode (AZO-MoS_2) shows a high responsivity of 40.67 A/W at 800 nm at low biasing voltage of 0.5 V. The self-driven behavior is observed in a broad range from 400 to 1100 nm with high responsivity of 38.18 mA/W at 800 nm. Moreover, AZO-MoS_2 device has fast rise and decay time. To understand impact of Ohmic AZO electrode in comparison to traditional metal electrodes, we have also investigated conventional Au-MoS_2 PDs fabricated under identical dimensions. The AZO-MoS_2 PD demonstrated 100 times higher responsivity than conventional Au-MoS_2 PD at 800 nm. We have investigated band-alignment between AZO and MoS_2 using ultraviolet spectroscopy (UPS) and confirmed ohmic nature between the AZO and MoS_2. These results indicate superior performance of AZO-MoS_2 PD device in comparison to traditional metal electrodes.
56.	Machine learning-based image processing in materials science and engineering: A review A Pratap, N Sardana - Materials Today: Proceedings, 2022 **Abstract**: Machine learning (ML) is playing a great role in every sphere of life including the area of materials science and engineering. At times, the experimental and computational data together create a complex scenario for interpretation giving rise to the requirement of ML. The incorporation of ML in the development of material science has a promised future to accelerate

	the research through automatic data interpretation with the help of different models like classification, Regression, Clustering, etc. Therefore, it becomes quick and easy to analyze the data sets with greater accuracy as compared to the analysis done by human researchers. This paper gives an overview of the applications and applicability of Machine Learning being used in various areas of materials development. The various image processing techniques which can be applied in material science are discussed in detail. In addition to that, the paper gives detail as to how a model can be trained with a smaller number of datasets. Subsequently, the different data ecosystems which can be useful for data collection and preparation before selecting any Machine Learning model are highlighted. Furthermore, the various opportunities and challenges that material scientists have been facing in the development of new materials are also outlined for a better understanding of ML-based image processing in material science and engineering.
57.	MDCADNet: Multi dilated & context aggregated dense network for non-textual components classification in digital documents M Singh, P Goyal - Expert Systems with Applications, 2022 **Abstract**: Non-Textual images like charts and tables are unlike natural images in various aspects, including high inter-class similarities, low intra-class similarities, substantial textual component proportions, and lower resolutions. This paper proposes a novel Multi-Dilated Context Aggregation based Dense Network (MDCADNet) addressing the multi-resolution and larger receptive field modeling need for the non-textual component classification task. MDCADNet includes a densely connected convolutional network for the feature map computation as front-end with a multi-dilated Backend Context Module (BCM). The proposed BCM generates multi-scale features and provides a systematic context aggregation of both low and high-level feature maps through its densely connected layers. Additionally, the controlled multi-dilation scheme offers a more extensive scale range for better prediction performance. A thorough quantitative evaluation has been performed on seven benchmark datasets for demonstrating the generalization capability of MDCADNet. Experimental results show MDCADNet performs consistently better than the state-of-the-art models across all datasets.
58.	Metal Additive Manufacturing: From History to Applications A Singh, H Singh - Innovations in Additive Manufacturing: Part of the Springer Tracts in Additive Manufacturing book series, 2022 **Abstract**: Additive manufacturing (AM), a new tool in the manufacturing toolbox, has hit the apex of the latest scenario of product developments. The technology is first recognized by Chuck Hull (co-founder of 3D systems) in 1987 that expended lightweight material for processing. However, the EOS introduced the first metal processed AM machine (EOSINT M160) to the market based on direct metal laser sintering (DMLS). Owing to the advantages offered, particularly the manufacturing of complex parts and reduction in product development steps, metal printers have gained considerable popularity among different industries. Consequently, numerous firms took part in commercializing their own AM technique with the respective proprietary names. The discussion on the type of various firms and their entry into AM market is elaborated under the history section. In the subsequent sections, the fundamental steps involved and essential aspects pertained to AM material compatibility are elucidated. Besides, the emphasis is given to AM techniques employed for metal/alloys processing. These AM technologies comprise powder bed fusion (PBF) process, powder fed fusion process and binder jetting technique. The mentioned processes are further sub-classified based on feedstock material and the energy source employed for consolidation. At last, the reader is introduced to the plethora of applications about metal AM in the manufacturing industries like aerospace,

	biomedical and automobile. In a nutshell, the basic idea behind this chapter is to provide an insight to the reader regarding the metal AM technology in terms of its history, material compatibility, fundamental steps, processing techniques and applications.
59.	Mining Social Networks for Dissemination of Fake News Using Continuous Opinion-Based Hybrid Model M Singh, SRS Iyengar, R Kaur - International Conference on Advanced Data Mining and Applications: Part of the Lecture Notes in Computer Science book series, 2022 **Abstract**: The entire world is confronting the challenge of fake news disseminated online, as its consequences could be exceptionally catastrophic. In this paper, we have proposed a hybrid model that integrates the opinion evolution process with the propagation of fake news. The level of extremity in opinions, the amount of support from social connections and the social influence were used as the major design considerations in modeling the spread of fake news. As polarized opinions on social media often lead to polarized networks, the proposed model was utilized to study the effect of evolving opinion on the spread of fake news on polarized networks of varying degrees. Our findings suggested that there are more users involved in sharing fake news in the presence of a highly polarized network. Moreover, the tendency of a user to adapt the opposing opinion seems to be correlated with the exposure of fake news. Besides this, we also assessed the consequences of the spread of fake news on the user's opinion and found that the users that are mainly influenced are the ones having an unclear stance towards a given issue. Overall, our proposed model highlights the interrelation between fake news and the opinion evolution on social networks.
60.	Modified KBBF-like Material for Energy Storage Applications: $ZnNiBO_3$ (OH) with Enhanced Cycle Life I Hussain, T Hussain, M Ahmad, X Ma, MS Javed… R Ahuja… - ACS Applied Materials & Interfaces, 2022 **Abstract**: Not only are new and novel materials sought for electrode material development, but safe and nontoxic materials are also highly being intensively investigated. Herein, we prepare $ZnNiBO_3$(OH) (ZNBH), a modified and Be-free $KBe_2BO_3F_2$ (KBBF) family member as an effective electrode material. The novel ZNBH resembles the KBBF structure but with reinforced structure and bonding, in addition to well-incorporated conductive metals benefiting supercapacitor applications. The enhanced electronic properties of ZNBH are further studied by means of density functional theory calculations. The as-prepared ZNBH electrode material exhibits a specific capacity of 746 C g^{-1} at a current density of 1 A g^{-1}. A hybrid supercapacitor (HSC) device is fabricated and successfully illuminated multiple color LEDs. Interestingly, even after being subjected to long charge–discharge for 10 000 cycles, the ZNBH//AC HSC device retains 97.2% of its maximum capacity, indicating the practicality of ZNBH as an electrode material. 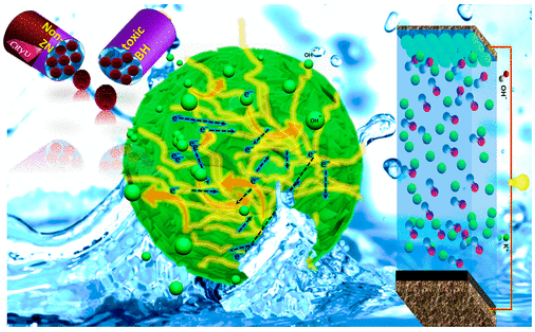

61.	New insights on MXene and its advanced hybrid materials for lithium-ion batteries J Jyoti, BP Singh, M Sandhu, SK Tripathi - Sustainable Energy & Fuels, 2022 **Abstract**: Electrode materials with exceptional cyclic stability and high-rate performance have been in extensive demand for the fast growth of energy storage applications. The focus of this article is on the recent progress, scientific challenges and future developments of advanced materials as anodes based on the two-dimensional (2D) MXene-based hybrid materials used in next generation lithium-ion batteries (LIBs). There is a big issue that extensively affects their performance, such as the restacking aggregation problem of MXene flakes. To address this issue, a basic and effective approach is to combine MXene with suitable and advanced materials, such as silicon, tin, different carbon nanofillers, metal oxide, phosphorous, metal sulphide and layered double oxide, to form the MXene hybrid composites. MXene surfaces have been modified in many ways, including decorating with silicon and tin-based nanoparticles, bridging networks with carbon nanofillers, and forming a heterostructure between graphene and MXene layers. The hybrid material has led to high ionic mobility, high diffusivity of Li+-ions, and electrical conductivity apart from specific capacity. In the current scenario, advanced electrode materials of LIBs should be highly promising to enhance the electrochemical performance of the batteries to make it more efficient than previously observed. The MXene-based hybrid nanostructure materials provide insight into future challenges and guidelines for finding new materials used in next-generation energy storage applications. 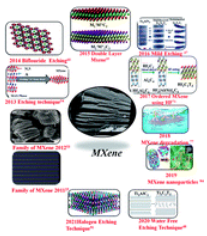
62.	Novel pulse compression favorable excitation schemes for infrared non-destructive testing and evaluation of glass fibre reinforced polymer materials A Rani, R Mulaveesala - Composite Structures, 2022 **Abstract**: Infrared thermography (IRT) has been extensively used in the field of non-destructive testing and evaluation (NDT&E) as a condition monitoring tool in commercial as well as industrial applications. It is a fast, non-contact, whole field and quantitative technique for NDT&E applications by mapping the thermal profile over the test sample. This paper presents a novel three-dimensional analytical model for characterization of glass fibre reinforced polymer (GFRP) sample having flat bottom hole defects. The capability of the proposed method is highlighted with recently introduced pulse compression favorable thermal wave imaging modalities. Further, the analytical results have been validated with simulated and experimental studies on the proposed frequency modulated thermal wave imaging (FMTWI), Barker coded thermal wave imaging (BCTWI) and digitized frequency modulated thermal wave imaging (DFMTWI) techniques to analyze the performance of the defect detectability by taking normalized correlation coefficient as a figure of merit. Obtained results clearly shows the capabilities of the DFMTWI over the FMTWI and BCTWI using correlation based matched filter post-processing approach.
63.	Numerical investigation of quenching technique for steel alloy hardening process using twins liquid jets SS Chandel, A Maurya, PK Singh - Materials Today: Proceedings, 2022

	Abstract: Quenching is one of the most common phenomena for hardening steel. The present study is focused on investigating the hardening of stainless-steel plates by single as well as twin liquid jets. To this end, flow interaction of twin jets on hot stainless-steel plate and consequent thermal characteristics (especially temperature profile) on the latter has been studied via commercial CFD software, ANSYS FLUENT 18. A steady-state, two- dimensional, and turbulent (standard k-epsilon) model has been developed by taking jet-based Reynolds number ranges between 3800 and 17,000 for the different nozzle to stainless steel plate distance, whereas the latter's temperature is fixed for 700 °C in the beginning. The results were compared with the help of stagnation heat transfer coefficient, stagnation Nusselt number, and turbulence effect near hot plate for the different nozzle to plate distance. Fluid interaction from twin jets also affects the cooling phenomena strongly, especially at the stagnation point. The local variation of heat transfer at the stagnation point was qualitatively different for different nozzle outlet velocity profiles near the plate.
64.	Occupation numbers and nuclear transition matrix elements for 0νβ−β− decay within a mechanism involving neutrino mass VK Nautiyal, R Gautam, N Das, R Chandra, PK Raina… - The European Physical Journal A, 2022 **Abstract**: By reproducing the experimentally available sub-shell occupation numbers of ^{100}Mo, ^{100}Ru, ^{128,130}Te, and ^{130}Xe nuclei, sets of four HFB intrinsic wave functions are generated with single particle energies due to Woods–Saxon potential and four different parametrizations of pairing plus multipolar effective two body interaction. In the rest of the considered nuclei, the single particle energies are scaled accordingly. Reliability of wave functions has been ascertained by comparing theoretically calculated and observed yrast spectra and deformation parameters β_2. Comparison between NTMEs $M^{-(K)}$ (K= 0ν and 0N) calculated with wave functions having adjusted and unadjusted occupation numbers shows that the former are in general reduced. Uncertainties in set of twelve nuclear transition matrix elements for the neutrinoless double-β decay of ^{94,96}Zr, ^{100}Mo, ^{110}Pd, ^{128,130}Te, and ^{150}Nd isotopes calculated using three different parametrizations of Jastrow short range correlations turn out to be 10–14% and 37% due to the exchange of light and heavy Majorana neutrino, respectively.
65.	On Learning Multi-UAV Policy for Multi-Object Tracking and Formation Control P Kaushik, A Garg, SS Jha - IEEE 18th India Council International Conference, 2021 **Abstract**: Autonomous navigation and formation control of multi-UAV systems poses a significant challenge for the robotic systems that operate in partially-observable, dynamic and continuous environments. This paper addresses the problem of multi-UAV formation control while cooperatively tracking a set of moving objects. The objective of the multi-UAV system is to maintain the moving objects under their joint coverage along with aligning themselves in an optimal formation for maximizing the overall area coverage. We develop a multi-agent reinforcement learning model to learn a cooperative multi-UAV policy for the multi-object tracking and formation control. We design a reward function to encode the objectives of tracking, formation and collision avoidance into the model. The proposed deep reinforcement learning based model is deployed and tested against a baseline controller using the Gazebo simulator. The result indicates that the proposed model is robust against the tracking and alignment errors outperforming the baseline model.
66.	Outage Analysis for Drone Assisted Multi-user Coded Cooperation P Kumar, S Bhattacharyya, S Darshi - IEEE 18th India Council International Conference, 2021

	Abstract: In the next generation wireless networks/systems, Drone Assisted Network Coded Cooperation (DA-NCC) aims to improve the reliability as well as throughput of the network. In this paper, we consider Non-Line-of-Sight (NLoS) environments and develop the theoretical framework for DA-NCC system by considering height dependent path loss exponent. For analysing the network performance, Amplify-and-Forward (AF) is used at relay for processing the signals and Selection Combining (SC) is used at destination nodes for combining the signals. To evaluate the network's performance, we formulated the expression of spectral efficiency and derived a mathematical equation of the outage probability for DA-NCC system. At the desired node, the mathematical equations for network coding noise, variance of network coding noise, and signal to overall noise ratio are also derived. To legitimize our analytical results, we use monte carlo simulations in MATLAB. In Vehicle-to-Vehicle (V2V) communications, smart cities, and disaster management, the generalized system model is useful for establishing reliable communication linkages among Ground Users (GUs) in the event that the central coordinator (Base Station (BS)) is disrupted.
67.	Performance and reliability improvement in intercalated MLGNR interconnects using optimized aspect ratio B Kumari, R Sharma, M Sahoo - Scientific Reports, 2022 **Abstract**: In this work, aspect ratio of various intercalation doped MLGNR interconnects are optimized using a numerical approach to achieve improved performance and reliability. A numerical optimization method is presented to estimate optimized aspect ratio considering combined effects of performance, noise and reliability metrics for any arbitrary nano interconnect system. This approach is cost effective and will be extremely useful to industry for selection of aspect ratio of interconnects as it is a non-SPICE method and reduces fabrication iterations for achieving desired performance and reliability. Our numerical method suggests that by minimizing the figure of merit (i.e. Noise Delay Power Product / Breakdown Power P_{BD} ratio), aspect ratio of FeCl3 doped MLGNR interconnect is optimized at 0.987, 0.61 and 0.579 for local, intermediate and global level, respectively at 7 nm node. Comparing the optimized performance metrics in this work with the estimated metrics at prescribed aspect ratio by IRDS roadmap, delay, noise delay product (NDP), power delay product (PDP), PDP/P_{BD} ratio and figure of merit are improved by (~2% and ~25%), (~44% and ~50%), (~9% and ~48%), (~6% and ~48%) and (~49% and ~68%) for 10 μ m and 1 mm long Fecl3 doped MLGNR interconnect, respectively at 7 nm node. Increase in contact resistance leads to significant decrease in performance and increase in optimized aspect ratio of local Fecl3 doped MLGNR interconnect. Scaling down from 10 to 7 nm node results in increase of optimized aspect ratio in all levels of interconnects. Even though the performance of MLGNR degrades with scaling down but when compared to copper, the performance improves with technology scaling. Finally, this study provides circuit designers a detailed guideline for selecting an optimized aspect ratio for achieving better performance, power efficiency and reliability in doped MLGNR interconnects.
68.	Postponement of dynamic Leidenfrost phenomenon during droplet impact of surfactant solutions GVVSV Prasad, P Dhar, D Samanta - International Journal of Heat and Mass Transfer, 2022 **Abstract**: In this article, a novel method of increasing the dynamic Leidenfrost temperature TDL is proposed by adding both anionic (SDS) and cationic (CTAB) surfactants to water droplets. We focus on understanding the hydrodynamics and thermal aspects of droplet impact Leidenfrost behavior of surfactant solutions and aim to delay the onset of the Leidenfrost regime. The effects of Weber number (We), Ohnesorge number (Oh), and surfactant concentration on dynamic

	Leidenfrost temperature (T_{DL}) were experimentally studied in detail, covering a wide gamut of governing parameters. At a fixed impact velocity, T_{DL} was increased with increase of surfactant concentration. T_{DL} decreased with the increase of impact velocity for all solutions of surfactant droplets at a fixed surfactant concentration. We proposed a scaling relationship for T_{DL} in terms of We and Oh. At temperatures (~ 400 °C) considerably higher than T_{DL}, droplets exhibit trampoline-like dynamics or central jet formation, associated with fragmentation, depending upon the impact velocity. Finally, a regime map of the different boiling regimes such as transition boiling, Leidenfrost effect, trampolining, and explosive behavior was presented as a function of impact We and substrate temperature (T_S). The findings may hold substantial implications in thermal management systems operating at high temperatures.
69.	Progressive Subtractive Recurrent Lightweight Network for Video Deraining A Kulkarni, PW Patil, S Murala - IEEE Signal Processing Letters, 2021 **Abstract**: Presence of rainy artifacts severely degrade the overall visual quality of a video and tend to overlap with the useful information present in the video frames. This degraded video affects the effectiveness of many automated applications like traffic monitoring, surveillance, etc. As video deraining is a pre-processing step for automated applications, it is highly demanded to have a lightweight deraining module. Therefore, in this paper, a "Progressive Subtractive Recurrent Lightweight Network" is proposed for video deraining. Initially, the Multi-Kernel feature Sharing Residual Block (MKSRB) is designed to learn different sizes of rain streaks which facilitates the complete removal of rain streaks through progressive subtractions. These MKSRB features are merged with previous frame output recurrently to maintain the temporal consistency. Further, multi-receptive feature subtraction is performed through Multi-scale Multi-Receptive Difference Block (MMRDB) to avoid loss of details and extract high-frequency information. Finally, progressively learned features through MKSRB and recurrent feature merging are aggregated with fused MMRDB features which outputs the rain-free frame. Substantial experiments on prevailing synthetic datasets and real-world videos verify the superior performance of the proposed method over the existing state-of-the-art methods for video deraining.
70.	Python-LTspice Co-Simulation to Train Neural Networks with Memristive Synapses to Learn Logic Gate Operations S Kumar, DM Das - IEEE International Symposium on Smart Electronic Systems, 2021 **Abstract**: Neuromorphic computing attempts to mimic the neural architecture of human brain by delivering a non vonNeumann hardware which can run even the most complex artificial intelligence algorithms at extremely fast computational speeds at power requirement as low in order as few tens of watts just like the human brain does. Since the brain is a complex mesh of millions of neurons communicating via the synapses and spiking signals in between them, there is a requirement of a circuit based memory element which can play the role of these synapses in electronic circuits. The memristors with there unique pinched hysteresis property have been proposed and modelled to act as these synapses. This paper introduces LTspice modelling of a simple artificial neural network with memristive synapses and training it for the universal gates-NOR and NAND by providing a mechanism for interpreting the compressed binary data generated by parametric LTspice simulations. The results show potential for application in many other crucial neuromorphic simulations and their numeric interpretation using the tool developed for Co-simulation of LTspice with the open source programming language, Python.

71.	Reactive power compensation for grid by Packed-U-Cell inverter using model predictive control strategy with intelligent multi-objective scheme M Anees, M Tariq, KA Lodi, M Alam… - Journal of Intelligent & Fuzzy Systems, 2022 **Abstract**: This paper proposes a model predictive control strategy for 15 level Packed-U-Cell inverter that satisfies multiple-objectives of low current total harmonic distortion (THD), capacitor voltage balances, supply of desired active and reactive power, as well as lower switching and lower voltage stresses on the switching devices. The proposed device performs well under dynamic conditions and can successfully track the current command during step changes in the power demand. A detailed modeling is presented and discussed. MATLAB/Simulink is used for obtaining the simulation results, and the results are validated in the real time by using a hardware-in-the-loop (HIL) Typhoon 402 real-time emulator.
72.	Relativistic Effects in Platinum Nanocluster Catalysis: A Statistical Ensemble-Based Analysis AS Nair, A Anoop, R Ahuja, B Pathak - The Journal of Physical Chemistry A, 2022 **Abstract**: Nanoclusters are materials of paramount catalytic importance. Among various unique properties featured by nanoclusters, a pronounced relativistic effect can be a decisive parameter in governing their catalytic activity. A concise study delineating the role of relativistic effects in nanocluster catalysis is carried by investigating the oxygen reduction reaction (ORR) activity of a Pt7 subnanometer cluster. Global optimization analysis shows the critical role of spin–orbit coupling (SOC) in regulating the relative stability between structural isomers of the cluster. An overall improved ORR adsorption energetics and differently scaled adsorption-induced structural changes are identified with SOC compared to a non-SOC scenario. Ab initio atomistic thermodynamics analysis predicted nearly identical phase diagrams with significant structural differences for high coverage oxygenated clusters under realistic conditions. Though inclusion of SOC does not bring about drastic changes in the overall catalytic activity of the cluster, it is having a crucial role in governing the rate-determining step, transition-state configuration, and energetics of elementary reaction pathways. Furthermore, a statistical ensemble-based approach illustrates the strong contribution of low-energy local minimum structural isomers to the total ORR activity, which is significantly scaled up along the activity improving direction within the SOC framework. The study provides critical insights toward the importance of relativistic effects in determining various catalytic activity relevant features of nanoclusters. 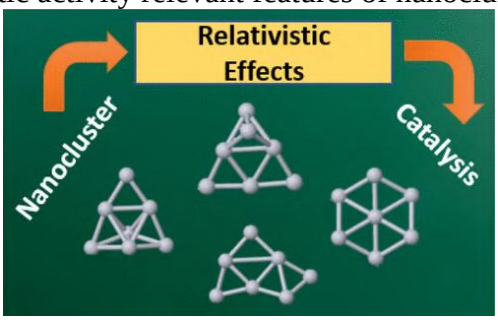
73.	Review of Voltage Regulation of a Doubly-Fed Induction Generator Based Wind Power Plant under Grid Faults P Khatri, KB Thapa, K Jayasawal, A Khanal, R Mahat - IEEE International Conference on Power Electronics, Smart Grid, and Renewable Energy, 2022 **Abstract**: The voltage at all buses in a power system should be kept constant in order to achieve voltage regulation. This manuscript evaluates various voltage regulation control schemes for a

	wind power plant (WPP) that uses a doubly-fed induction generator (DFIG). These regulation schemes are particularly appropriate in injecting the reactive power to fortify the voltage at the point of interconnection (POI) throughout a disturbance without using external devices such as flexible AC transmission system (FACTS) devices in a WPP. The control schemes employed in the DFIG and WPP controllers are reviewed, and all the control schemes employed in them are also classified. DFIG controllers are operated in the voltage control, reactive power, and reactive current control modes whereas the WPP controller either activates in reactive power control or voltage control modes. Based on the classification, this paper depicts the merits and demerits of each control scheme, compares them, and also shows broad space for further research. The comparative results are likely to be useful to researchers and engineers involved in the field of voltage regulation of DFIG-based WPP.
74.	Role of Au–Ag alloy plasmonic layer thickness over pyramidal silicon in controlling SERS activity S Midha, S Jain, S Sarkar - The European Physical Journal Special Topics, 2022 **Abstract**: In this study, we systematically explore the role played by thickness of SERS functional metallic plasmonic layer over pyramidal Si pre-templates in controlling the SERS behavior. For this purpose, three different thicknesses, i.e., 30, 50, and 70 nm, of Au–Ag alloy nanolayer were investigated over topographically variant pyramidal Si templates. The fabrication of pyramidal templates was followed using a simple and cost-intensive anisotropic wet chemical etch approach by having a variation in etching time. The SERS response of R6G dye probe molecule on these substrates shows a strong dependence on both thickness and template topography. A substantially high SERS contribution comes from the 50 nm-thick film over a surface with dense and small pyramids. An enhancement factor of 8.6 ×106 is observed for this case. Finally, a suitable thickness is proposed for a better SERS response. This work suggests a significant role of thickness in designing potential SERS substrates.
75.	Scattering of water waves by very large floating structure in the presence of a porous box S Singla, H Behera, SC Martha, T Sahoo - Journal of Offshore Mechanics and Arctic Engineering, 2022 **Abstract**: We investigate the effectiveness of a porous box in attenuating the structural response of a very large floating structure (VLFS). Assuming the water depth to be finite and small amplitude water wave theory, the physical problem is formulated by employing Darcy's law for flow past a porous structure. The boundary value problem is reduced to a system of linear algebraic equations with the aid of matched eigenfunction expansion method. Further, these simultaneous equations are solved numerically to compute physical quantities. The mathematical model is validated through a comparison with the theoretical results available in the literature. The elastic plate deflection, forces acting on the box and free surface elevation are computed. The efficiency of the given system in transmitting, reflecting and dissipating the incident wave energy is analysed through various graphs. The study reveals that the width and height of the porous box are critical towards the trapping of incident waves inside the box and dissipating the maximum amount of incident wave energy in reduction of wave transmission in the lee side of the structure and thereby attenuating the structural response of the VLFS.
76.	Semi-Empirical Models for Temperature and Electric Field Dependent Complex Permittivity of Solid Dielectrics P Johri, CC Reddy - IEEE Conference on Electrical Insulation and Dielectric Phenomena, 2021 **Abstract**: In this paper, the authors present models for the temperature and electric field

	dependence of AC complex permittivity of solid dielectrics used for power cables. Until now, variation in permittivity, with temperature and field, has been more or less neglected. Although small, both real and imaginary components of the complex AC permittivity are somewhat nonlinear in nature and thus, determination of true behavior of the dielectric requires accurate modelling of the complex AC permittivity. Careful and intensive experimental investigations are carried out using Novocontrol Technologies' broadband dielectric spectrometer, for different temperatures and electric fields and constant frequency of 50Hz and the data is used for curve fitting and subsequent optimization. The suitability of the proposed models has been verified for two different dielectrics. Interesting results on coefficients of the models have been arrived at, that provide deeper insight into the dielectric behaviour.
77.	Shape Coexistence in Proton Rich Se Isotopes A Mukherjee, S Bhattacharya, T Trivedi, RP Singh… D Choudhury… - Bulgarian Journal of Physics, 2022 **Abstract**: The structural features of the ^{72}Se nucleus, obtained from our recent work [1], have been compared with the neighboring even-even proton rich Se isotopes to get a better understanding about the presence of shape coexistence at low spin states. The corresponding alignment behaviour of different Se isotopes has been used to understand the shapes of the coexisting states at low excitation energy. The experimental results of Se isotopes have been interpreted in the framework of total Routhian surface (TRS) calculations.
78.	Software-Defined Networking in Data Centers P Kamboj, S Pal - Software Defined Internet of Everything: Part of the Internet of Things book series, 2022 **Abstract**: Cloud computing and software-defined networking (SDN) have gained a lot of interest from industry and academia. With the increase in data from applications, data centers require high-speed access networks to fulfill the user demands. Today, the data centers are facing scalability challenges and do not adapt to dynamic application requirements. However, features in SDN facilitate data processing, storage, and transmission of data center applications. This chapter presents an overview of SDN's importance in cloud computing and to overcome the challenges in data centers. Further, we discuss how SDN in data center networks benefits for managing routing, traffic engineering, and resource management. Moreover, we also present the different methods that have been adopted for SDN-based energy-aware routing strategies to minimize power consumption in data centers.
79.	State-Of-Art Machine Learning Techniques to Predict Airlines Delay S Sharan, M Sriniketh, H Vardhan, D Jayanth - International Conference on Forensics, Analytics, Big Data, Security, 2021 **Abstract**: Nowadays everyone is becoming extremely busy that makes them follow the time very precisely. In the commercial aviation sector, flight delays are a significant cause of dissatisfaction with customers. So, the prediction of flight delays plays a pivotal role in travelers' comfort and alleviates the airline's economic losses. This paper analyzes the performance of the machine learning algorithms such as Random Forest, AdaBoost, and XGBoost classifier to handle the delay time prediction of flight by considering multiple parameters such as weather conditions, flight schedule, etc., that are responsible for flight delay. The paper does a detailed comparative analysis of the algorithms used. Our study can also be applied to various other applications, such as predicting demand-based airline fares.
80.	Strain-mediated ferromagnetism and low-field magnetic reversal in Co doped monolayer WS_2

	AK Jena, SK Mallik, MC Sahu, S Sahoo, AK Sahoo…R Ahuja… - Scientific Reports, 2022 **Abstract**: Strain-mediated magnetism in 2D materials and dilute magnetic semiconductors hold multi-functional applications for future nano-electronics. Herein, First principles calculations are employed to study the influence of biaxial strain on the magnetic properties of Co-doped monolayer WS_2. The non-magnetic WS_2 shows ferromagnetic signature upon Co doping due to spin polarization, which is further improved at low compressive (-2 %) and tensile (+2 %) strains. From the PDOS and spin density analysis, the opposite magnetic ordering is found to be favourable under the application of compressive and tensile strains. The double exchange interaction and p-d hybridization mechanisms make Co-doped WS_2 a potential host for magnetism. More importantly, the competition between exchange and crystal field splittings, i.e. ($\Delta_{ex}>\Delta_{cfs}$), of the Co-atom play pivotal roles in deciding the values of the magnetic moments under applied strain. Micromagnetic simulation reveals, the ferromagnetic behavior calculated from DFT exhibits low-field magnetic reversal (190 Oe). Moreover, the spins of Co-doped WS_2 are slightly tilted from the easy axis orientations showing slanted ferromagnetic hysteresis loop. The ferromagnetic nature of Co-doped WS_2 suppresses beyond ±2 % strain, which is reflected in terms of decrease in the coercivity in the micromagnetic simulation. The understanding of low-field magnetic reversal and spin orientations in Co-doped WS_2 may pave the way for next-generation spintronics and straintronics applications.
81.	Strain modulating electronic band gaps and SQ efficiencies of semiconductor 2D PdQ2 (Q= S, Se) monolayer D Raval, SK Gupta, PN Gajjar, R Ahuja - Scientific Reports, 2022 **Abstract**: We studied the physical, electronic transport and optical properties of a unique pentagonal PdQ_2 (Q = S, Se) monolayers. The dynamic stability of 2Dwrinkle like-PdQ_2 is proven by positive phonon frequencies in the phonon dispersion curve. The optimized structural parameters of wrinkled pentagonal PdQ_2 are in good agreement with the available experimental results. The ultimate tensile strength (UTHS) was calculated and found that, penta-PdS_2 monolayer can withstand up to 16% (18%) strain along *x* (*y*) direction with 3.44 GPa (3.43 GPa). While, penta-$PdSe_2$ monolayer can withstand up to 17% (19%) strain along *x* (*y*) dirrection with 3.46 GPa (3.40 GPa). It is found that, the penta-PdQ_2 monolayers has the semiconducting behavior with indirect band gap of 0.94 and 1.26 eV for 2D-PdS_2 and 2D-$PdSe_2$, respectively. More interestingly, at room temperacture, the hole mobilty (electron mobility) obtained for 2D-PdS_2 and $PdSe_2$ are 67.43 (258.06) $cm^2 V^{-1} s^{-1}$ and 1518.81 (442.49) $cm^2 V^{-1} s^{-1}$, respectively. In addition, I-V characteristics of $PdSe_2$ monolayer show strong negative differential conductance (NDC) region near the 3.57 V. The Shockly-Queisser (SQ) effeciency prameters of PdQ_2 monolayers are also explored and the highest SQ efficeinciy obtained for PdS_2 is 33.93% at −5% strain and for $PdSe_2$ is 33.94% at −2% strain. The penta-PdQ_2 exhibits high optical absorption intensity in the UV region, up to 4.04×10^5 (for PdS_2) and 5.28×10^5 (for $PdSe_2$), which is suitable for applications in optoelectronic devices. Thus, the ultrathin PdQ_2 monolayers could be potential material for next-generation solar-cell applications and high performance nanodevices.
82.	Supersolid-like solitons in a spin-orbit-coupled spin-2 condensate P Kaur, S Gautam, SK Adhikari - Physical Review A, 2022 **Abstract**: We study supersolid-like crystalline structures emerging in the stationary states of a quasi-two-dimensional spin-orbit (SO)-coupled spin-2 condensate in the ferromagnetic, cyclic, and antiferromagnetic phases by solving a mean-field model. Interplay of different strengths of

	SO coupling and interatomic interactions gives rise to a variety of nontrivial density patterns in the emergent solutions. For small SO-coupling strengths γ ($\gamma \approx 0.5$), the ground state is an axisymmetric multiring soliton for polar, cyclic, and weakly ferromagnetic interactions, whereas for stronger ferromagnetic interactions a circularly asymmetric soliton emerges as the ground state. Depending on the values of interaction parameters, with an increase in SO-coupling strength, a stripe phase may also emerge as the ground state for polar and cyclic interactions. For intermediate values of SO-coupling strength ($\gamma \approx 1$), in addition to these solitons, one could have a quasidegenerate triangular-lattice soliton in all magnetic phases. On further increasing the SO-coupling strength ($\gamma \gtrapprox 4$), a square-lattice and a superstripe soliton emerge as quasidegenerate states. The emergence of all these solitons can be inferred from a study of solutions of the single-particle Hamiltonian.
83.	Sustainable cooling strategies to reduce tool wear, power consumption and surface roughness during ultrasonic assisted turning of Ti-6Al-4V J Airao, CK Nirala, R Bertolini, GM Krolczyk, N Khanna - Tribology International, 2022 **Abstract**: Issues related to the machinability of difficult-to-machine materials such as Titanium and Nickel base superalloys are well explicated in the literature. In this regard, a novel study, applying ultrasonic vibration along with MQL and LCO_2, is proposed to enhance the machinability of Ti-6Al-4V. In this regard, this article attempts to analyze machinability of Ti-6Al-4V in conventional and Ultrasonic Assisted Turning (UAT) under dry, wet, MQL and LCO_2. The experiments are performed on an in-house developed ultrasonic assisted turning setup, keeping all the machining parameters constant. The main tool wear mechanisms observed are diffusion, adhesion, abrasion, and built-up edge formation in both cutting strategies. Moreover, the LCO_2 and ultrasonic vibration significantly reduce specific cutting energy without compromising the surface roughness and tool life. Ultimately, the LCO_2, along with ultrasonic assisted turning, promotes sustainability in the machining of Ti-6Al-4V.
84.	Sustainable Synthesis of Ionic Liquid-Functionalized Zinc Oxide Nanosheets (IL@ZnO): Evaluation of Antibacterial Potential Activity for Biomedical Applications D Bains, G Singh, N Singh - ACS Applied Bio Materials, 2022 **Abstract**: Zinc oxide (ZnO)-derived materials exhibit unique antibacterial, antifungal, and photochemical activities and are widely used in antibacterial formulations. In this work, ZnO nanosheets were prepared by green and cost-effective synthesis via a hydrothermal method, and the prepared ZnO nanosheets were further functionalized with an eco-friendly ionic liquid (IL). Thus, a sustainable approach was established to synthesize ZnO nanosheets. The functionalization of ZnO with the synthesized IL was fully characterized by advanced spectroscopic and microscopic techniques. The prepared ionic liquid-functionalized ZnO (IL@ZnO) showed self-organized layered-sheet arrangements caused by the intercalation of the IL onto the surface of ZnO nanosheets as revealed by scanning electron microscopy (SEM). The design of the IL comprised a carboxylic acid moiety for functionalization onto the surface of ZnO, whereas the hydrophobicity was tuned through the incorporation of a long alkyl chain. The developed IL@ZnO material was also tested against both Gram-positive and Gram-negative pathogenic bacteria for potential antibacterial activity by colony-forming unit (CFU) and minimum inhibitory concentration tests. The results revealed that the IL@ZnO exhibits significant antibacterial activity against tested strains. In particular, potent activity was observed against the Gram-positive skin-specific Staphylococcus aureus bacteria strain. The mechanism of bactericidal activity against bacteria was also explored along with the cytotoxicity toward mammalian cells, which reveals that the IL@ZnO is nontoxic in nature. To utilize the developed

	material owing to its bactericidal activity for practical applications, the IL@ZnO was fabricated onto the surface of cotton fabric, and its surface morphology was examined by SEM; the activity of IL@ZnO-treated cotton fabric was evaluated by the zone of inhibition assay. Additionally, the IL@ZnO-treated cotton fabric exhibited remarkable stability along with significant hydrophobicity and breathability and thus can be utilized as a biomaterial for biomedical applications, especially in medical masks, for reducing the risk of transmission of infectious diseases. 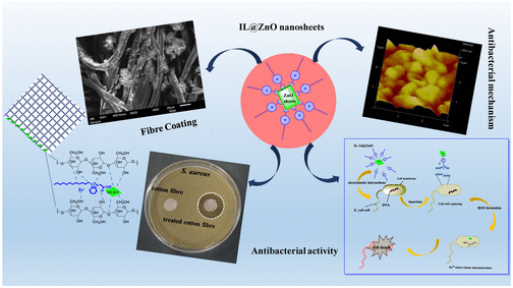
85.	The Legacy of Scatterometers: Review of Applications and Perspective S Singh, RK Tiwari, V Sood, R Kaur… - IEEE Geoscience and Remote Sensing Magazine, 2022
86.	THERMOD: Development of a Cost Effective Solution for Integrated Sensing and Logging LK Baghel, VK Malav, S Kumar - IEEE Sensors Journal, 2022 **Abstract**: With the outbreak of the Covid-19 pandemic, vaccination has become mandatory. Further, for effective results, the vaccines should be stored within the recommended temperature range, typically between 2°C to 8°C, transported safely without any mishandling and temperature excursion. In order to assure vaccine potency, it is essential to have detailed information on the entire temperature data recorded at user-defined intervals. In this paper, we develop functionality interaction to bring different sensors, memory, and processing units to an integrated platform, providing a compact, power-efficient, and low-cost commercial TemperatuRE, Humidity, and MOvement Data-logger (THERMOD). Moreover, the THERMOD hardware is packed with interactive algorithms that address the aforementioned concerns and log the real-time temperature and jerks (3-dimensional movement) encountered throughout the journey, and the logged data can be retrieved by plugging THERMOD into the host computer/laptop. The THERMOD hardware formulation and algorithm embedding have been done in the institution lab, which enables end-to-end storage and monitoring. Also, the proposed design is built with the defined standards by health organizations, e.g., WHO. Further, to validate the proficiency of the proposed design, comparative analysis has been done; a) a cost analysis has been done to state the cost efficiency of the proposed solution, b) real-time power performance graphs have been plotted which depict that THERMOD outperforms the existing solutions. Moreover, a number of experiments were performed for the validation of the proposed design.
87.	Thermodynamic Analysis of the Volumetric Absorption Solar Collector driven Direct Contact Membrane Distillation System K Garg, A Rathore, R Yadav, SK Das, H Tyagi - Journal of Thermal Science and Engineering Applications, 2022 **Abstract**: Solar-powered membrane distillation (SP-MD) technology has proven to be an ideal solution for providing fresh water in remote and off-grid locations. In this study, a novel solar energy-driven direct contact membrane distillation (DCMD) cycle is proposed in which a nanofluid-based volumetric absorption solar collector (VASC) is used to drive the DCMD

	process. The present work focuses on the use of volumetric collector instead of commercially available surface absorption-based solar collector in case of two-loop indirect SP-MD systems which are installed to control the scaling and corrosion issues in solar collectors. The thermodynamic performance of this two-loop indirect SP-DCMD system has been evaluated with the help of a mathematical model prepared in MATLAB. For modeling the DCMD unit, ε-NTU method used for designing heat exchangers has been employed. The performance of the overall system is evaluated by gained output ratio (GOR), thermal efficiency (η) of the membrane distillation, and water flux (Jw) and effect of various operating parameters related to both DCMD and VASC systems have been understood on the overall system performance. Finally, it has been shown that VASC driven DCMD system has approximately 4-15% higher gained output ratio as compared to SASC driven DCMD system under similar operating conditions.
88.	Transient Electric and Thermal Fields in a HVDC cable S Dhayalan, BS Thind, CC Reddy - IEEE Conference on Electrical Insulation and Dielectric Phenomena, 2021 **Abstract**: Polymeric insulation is being widely used in HVDC cables owing to its several advantages. The performance of a HVDC cable during transients, such as sudden switching and polarity reversal etc., will not be the same as in steady state. In this work the design performance of a HVDC cable has been evaluated. During transient periods the cable insulation suffers from high electro-thermal stress. In this paper, an electro-thermal model has been considered for simulation. The nonlinear DC conductivity is experimentally measured and incorporated in the model to analyze exact performance of cable as per Cigré standard TB 496. The electric field, temperature distribution and insulation leakage current have been analyzed. Peak electric field and field enhancement factors are obtained.
89.	Two-Dimensional Bismuthene Nanosheets for Selective Detection of Toxic Gases P Panigrahi, PK Panda, Y Pal, H Bae, H Lee, R Ahuja… - ACS Applied Nano Materials, 2022 **Abstract**: An in-depth understanding of the practical sensing mechanism of two-dimensional (2D) materials is critically important for the design of efficient nanosensors toward environmentally toxic gases. Here, we have performed van der Waals-corrected density functional theory (DFT) simulations along with nonequilibrium Green's function (NEGF) to investigate the structural, electronic, transport, thermodynamic, and gas-sensing properties of pristine and defect-crafted bismuthene (bBi) sheets toward sulfur- (H2S, SO2) and nitrogen-rich (NH3, NO2) toxic gases. It is revealed that the electrical conductivities of pristine and defective bBi sheets are altered upon the adsorption of incident gases, which have been verified through transport calculation coupled with the work function and electronic density of states. Our calculations disclose that bBi sheets show superior and selective gas-sensing performance toward NO2 molecules among the studied gases due to a significant charge redistribution and more potent adsorption energies. We find that the mono- and divacancy-induced bBi sheets have enhanced sensitivity because the adsorption behavior is driven by a considerable change in the electrostatic potential difference between the sheets and the gas molecules. We further performed statistical thermodynamic analysis to quantify the gas adsorption abilities at the practical temperature and pressures for the studied gas samples. This work divulges the higher sensitivity and selectivity of bBi sheets toward hazard toxins such as NO2 under practical sensing conditions of temperature and pressure.

	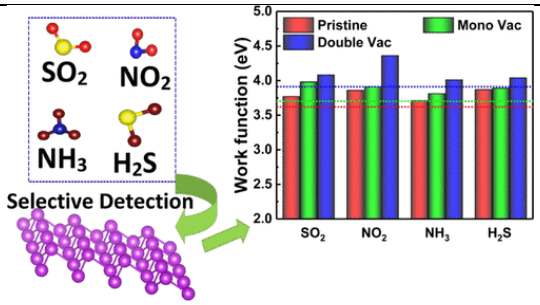
90.	Two-Dimensional Perovskite/HfS_2 van der Waals Heterostructure as an Absorber Material for Photovoltaic Applications D Singh, R Ahuja - ACS Applied Energy Materials, 2022 **Abstract**: Van der Waals (vdW) heterostructures of perovskites and transition metal dichalcogenides (TMDCs) have attracted increased interest owing to their extraordinary optoelectronic properties and encouraging applications. Two-dimensional (2D) TMDCs, i.e., hafnium disulfide (HfS_2), are also interesting because of their unique optoelectronic properties. Therefore, the combination of these different types of materials is very smart in terms of the fundamental science of interface interaction, as well as for the understanding of ultrathin optoelectronic devices with superior performance. Here, we have systematically modeled the 2D $CH_3NH_3PbI_3/HfS_2$ vdW heterostructure by using first-principles calculations. The substituted interface has enhanced visible-light sensitivity and photoelectrocatalytic activity by reducing the transition energies. The interfacial interaction of both materials effectively tunes the band gap of the interface; therefore, it would significantly improve the photoreactivity for solar cell applications. Due to the presence of small effective masses of electrons–holes, high optical absorption on the order of 105 and high spectroscopic limited maximum efficiency of 28.45% in the $CH_3NH_3PbI_3/HfS_2$ vdW heterostructure will be better candidates in the field of absorber materials. The considered systems are expected to be more efficient in separating the photogenerated electrons–holes and active in the visible spectrum. These theoretical results suggest that the $CH_3NH_3PbI_3/HfS_2$ vdW heterostructure may lead to many novel applications in efficient light-absorbing materials for photovoltaic applications.

Disclaimer: This publication digest may not contain all the papers published. Library has compiled the publication data as per the alerts received from Scopus and Google Scholar for the affiliation “Indian Institute of Technology Ropar” for the month of February 2022. The author(s) are requested to share their missing paper(s) details if any, for the inclusion in the next publication digest.